ISTANBUL TECHNICAL UNIVERSITY ★ GRADUATE SCHOOL OF SCIENCE ENGINEERING AND TECHNOLOGY

DEVELOPING 3D-PRINTABLE HIGH PERFORMANCE POLYMER COMPOSITES FOR THERMAL MANAGEMENT APPLICATIONS

M.Sc. THESIS

Yunus Emre BOZKURT

Department of Defence Technologies

Defence Technologies Programme

JULY 2020

ISTANBUL TECHNICAL UNIVERSITY ★ GRADUATE SCHOOL OF SCIENCE ENGINEERING AND TECHNOLOGY

DEVELOPING 3D-PRINTABLE HIGH PERFORMANCE POLYMER COMPOSITES FOR THERMAL MANAGEMENT APPLICATIONS

M.Sc. THESIS

Yunus Emre BOZKURT
(514181018)

Department of Defence Technologies

Defence Technologies Programme

Thesis Advisor: Assoc. Prof. Hülya CEBECİ

JULY 2020

İSTANBUL TEKNİK ÜNİVERSİTESİ ★ FEN BİLİMLERİ ENSTİTÜSÜ

3B-BASILABILIR YÜKSEK PERFORMANSLI POLİMER KOMPOZİTLERİN TERMAL YÖNETİM SİSTEMLERİ İÇİN GELİŞTİRİLMESİ

YÜKSEK LİSANS TEZİ

Yunus Emre BOZKURT
(514181018)

Savunma Teknolojileri Anabilim Dalı

Savunma Teknolojileri Programı

Tez Danışmanı: Doç. Dr. Hülya CEBECİ

TEMMUZ 2020

Yunus Emre BOZKURT, a M.Sc. student of ITU Graduate School of Science Engineering and Technology 514181018 successfully defended the thesis entitled "DEVELOPING 3D-PRINTABLE HIGH PERFORMANCE POLYMER COMPOSITES FOR THERMAL MANAGEMENT APPLICATIONS", which he prepared after fulfilling the requirements specified in the associated legislations, before the jury whose signatures are below.

Thesis Advisor :	**Assoc. Prof. Hülya CEBECİ** Istanbul Technical University	.....
Jury Members :	**Assoc. Prof. Hülya CEBECİ** ISTANBUL Technical University	.....
	Prof. Yusuf MENCELOĞLU SABANCI University	.....
	Prof. Halit S. TÜRKMEN ISTANBUL Technical University	.....

Date of Submission : **15 June 2020**
Date of Defense : **24 July 2020**

To my lovely mother,

FOREWORD

First, I am grateful to my advisor Assoc. Prof. Hülya Cebeci for the guidance, support and advises giving me needful guidance to complete this thesis. This thesis would not have been possible without her constructive criticisms.

I am also grateful to The Boeing Company for supporting this work financially. I also would like to thank Özlem Türkarslan (Ph.D.), Feride N. Şaşal, Travis Sherwood and Arun Muley (Ph.D.) for their valuable discusions on my work.

Also, I would like to specially thank Alptekin Yıldız (Ph.D.) for sharing his knowledge and collaboration. Moreover, I am grateful to Kaan Yıldız (Ph.D.) for his recommendations during writing the thesis. Also, special thanks to my friends, Uğur Emanetoğlu, Elçin Akar, Fulden Kaygınok and Suat Ebil for their helps and colleagues in Nanomaterials, Textiles and Advanced Composites Research Group in Aerospace Research Center, Istanbul Technical University.

I am grateful to Assist. Prof. Nuri Solak, Cem Kıncal and Gürkan Koçsız for his help in thermal conductivity measurements.

I am especially thankful to Rojda Şara for her encouragement and belief in me.

Also, I am greatly thankful my father Ali Bozkurt, my mother Gülüşan Bozkurt and my sister Mevlüde Bozkurt for their support, encouragement and motivation.

July 2020

Yunus Emre BOZKURT
Metallurgical and Materials Engineer

Not subject to U.S. Export Administration Regulations (EAR), (15 C.F.R. Parts 730-774) or U.S. International Traffic in Arms Regulations (ITAR), (22 C.F.R. Parts 120-130).

TABLE OF CONTENTS

Page

ABBREVIATIONS

3D	**:** Three Dimensional
ABS	**:** Acrylonitrile Butadiene Styrene
AM	**:** Additive Manufacturing
CAD	**:** Computer-aided Design
CNT	**:** Carbon Nanotube
CTE	**:** Coefficient of Thermal Expansion
DSC	**:** Differential Scanning Calorimetry
FFF	**:** Fused Filament Fabrication
h-BN	**:** Hexagonal Boron Nitride
HDPE	**:** High Density Polyethylene
PC	**:** Polycarbonate
PEEK	**:** Polyetherether Ketone
PEI	**:** Polyetherimide
PLA	**:** Polylactic acid
PMC	**:** Polymer Matrix Composite
PPS	**:** Polyphenylene Sulphide
RP	**:** Rapid Prototyping
SEM	**:** Scanning Electron Microscopy
Tg	**:** Glass Transition Temperature
TGA	**:** Thermogravimetric Analysis
TIM	**:** Thermal Interface Material

SYMBOLS

W	**:** Watt
K	**:** Kelvin
m	**:** Meter
Pa	**:** Pascal
$\dot{\gamma}$	**:** Shear Rate
$\mathbf{G}'$	**:** Storage Modulus
$\mathbf{G}''$	**:** Loss Modulus
η^*	**:** Complex Viscosity

LIST OF TABLES

Page

LIST OF FIGURES

Page

DEVELOPING 3D-PRINTABLE HIGH PERFORMANCE POLYMER COMPOSITES FOR THERMAL MANAGEMENT APPLICATIONS

SUMMARY

Energy created by electronic devices has caused many problems such as thermal stress and exceeding operating temperature in electronic applications. Thermal dissipation of created heat energy has become a critical problem in recent years due to the appearance of new devices and the functionalization of electronics. To meet the demand for high heat capacity materials in the new emerging technologies and overcome the issues of conventional materials, such as high thermal expansion coefficients, low corrosion resistance, and high production cost, development of novel polymer composite materials with enhanced thermal conductivities is needed. Rather than conventional metals, polymers with their lightweight and corrosion resistance properties can be an alternative for next-generation heat exchangers. However, fundamental challenges may arise for polymers, for example, several thermoplastics suffer from low mechanical strength, physical aging, low service temperature, and difficult processability. Hence, novel polymer composites reinforced with fillers that exhibit high thermal conductivity and mechanical strength may be an alternative solution for next-generation heat exchangers and thermal interface materials utilizing a careful approach in design and manufacturing. However, compared to metals, commodity polymers exhibit substantially lower thermal conductivities. Because of that, to evaluate the potential of thermoplastics as a lightweight alternative, the detailed examination should be performed to establish the effective phonon transport mechanisms. Therefore, incorporating nano or micro-fillers to high-performance polymers can help overcome challenges arisen from low thermal conductivity of thermoplastics with a minimal weight penalty.

Additive Manufacturing which is also known as three-dimensional (3D) printing or rapid prototyping (RP), is a novel technology for fabrication of the objects that may come in complex shapes. Fused filament fabrication (FFF) technique is one of the most widely used techniques to fabricate polymer composites thanks to its advantages such as cost efficiency, high production speed, and simplicity. Thermoplastic polymers such as polylactic acid (PLA), acrylonitrile butadiene styrene (ABS), polycarbonate (PC), polyetherimide (PEI), polyetherether ketone (PEEK), and polyphenylene sulfide (PPS) are commonly used as feedstock materials in the FFF technique. FFF technique suffers from mainly two difficulties which are limited feedstock materials requiring suitable viscosity and the need to have the feedstock in filament form. Therefore, suitable polymers should be fabricated for their use in the FFF.

This thesis is based on developing a high performance polymer composite filament for 3D printing with a high thermal conductivity for advanced in aerospace and defence fields. In this context, PEI was chosen as polymer material with its high mechanical properties, and operating temperature. PEI is reinforced by hexagonal boron nitride (h-BN) as a ceramic-based additive and carbon nanotubes (CNTs) as a carbon-based

additive to increase thermal conductivity of base polymer matrix for the targeted applications such as heat exchangers and/or thermal interface materials.

First, a parametric study to optimize the rotor speed, temperature and feeding rate conditions for achieving a proper dispersion state of BN as a filler in an amorphous high-performance polymer, PEI was performed. To minimize the interfacial phonon scattering mechanism, and tune the processing-dispersion and dispersion-thermal conductivity relation, BN/PEI polymer composites were fabricated with different rotor speeds (from 50 rpm to 330), at various feeding rates (from 0.5 kg/h to 1.5 kg/h) and temperatures between 350 °C to 380 °C. Then, fabricated polymer composites were investigated by rheological analysis to determine proper working conditions. As a result of these measurements, the optimum process conditions for BN/PEI polymer composites fabrication were determined as 250 rpm rotor speed, 1 kg/h feeding rate, and 360 °C die temperature.

Fabrication of BN/PEI composites were carried out based on optimum processing conditions and 5, 10, 15, 20, 25, and 30 weight (wt.) %BN was added into PEI matrix. Then, 1, 2, and 5 wt.% CNTs were added into BN/PEI to form the hybrid polymer composites as filament.

BN/PEI and CNTs/BN/PEI composites were characterized by thermogravimetric analysis (TGA), differential scanning calorimetry (DSC), rheometry, and thermal conductivity measurements. TGA results demonstrated that BN and CNTs addition led to an increase in starting temperatures of thermal decomposition of PEI. DSC analysis showed that BN, CNTs addition did not lead to change in glass transition temperatures of PEI. Rheological measurements revealed that flow behaviour of PEI was changed remarkably with 15 wt. %BN and 1 wt. %CNTs additions and these amounts were determined as percolation thresholds.

To measure the thermal conductivity of BN/PEI and CNTs/BN/PEI composites, cylindrical discs were fabricated by two methods as: (i) 3D printer process, and (ii) hot-press process to make suitable for thermal conductivity measurements. Thermal conductivity results showed that compared to neat PEI 30 wt. %BN addition into PEI matrix led to a 289% increase in thermal conductivity by reaching 0.82 W/m K. Besides, compared to neat PEI 5 wt. %CNTs addition into 20 wt. %BN/PEI composites led to a 389% increase in thermal conductivity by reaching 1.03 W/m K.

In conclusion, within the scope of this thesis the effects of BN and CNTs on the thermal conductivity and flow properties of PEI were investigated and 3D printed thermal conductive polymer composites were fabricated successfully.

3B-BASILABILIR YÜKSEK PERFORMANSLI POLİMER KOMPOZİTLERİN TERMAL YÖNETİM SİSTEMLERİ İÇİN GELİŞTİRİLMESİ

ÖZET

Son yıllarda daha küçük hacimlerde daha fazla işlem yapmaya imkan sağlayan mikro çipler gibi cihazlar yer aldıkları uygulamaların etkili bir şekilde çalışmasını sağlamasının yanı sıra daha fazla enerji tüketmekte ve buna bağlı olarak cihazlardan yayılan ısıyı artırmaktadır. Özellikle havacılık, savunma, enerji ve otomotiv sanayinde tercih edilen bu cihazlar içinde bulundukları yapının etkili bir şekilde soğutulması ihtiyacını da beraberinde getirmektedir. Bu soğutma işlemleri, genellikle soğutucu ve ısı değiştirici olarak adlandırılan uygulamalar ile yapılmaktadır. Bu uygulamalar için genellikle yüksek ısı iletkenliklerine sahip olmaları sebebiyle bakır ve alüminyum gibi metal malzemeler kullanılmaktadır. Metal malzemeler, yüksek genleşme kat sayıları, yüksek yoğunlukları, düşük korozyon dirençleri, ve yüksek üretim maaliyetleri sebebi ile uygulamaları sırasında sorunlara yol açmaktadır. Bu nedenlerle, termal yönetim uygulamalarında kullanılmak üzere polimer malzemelerin geliştirilmesi önem kazanmaktadır.

Eklemeli imalat olarak adlandırılan üretim yöntemlerinden birisi olan Eriyik Biriktirmeli Modelleme yöntemi termoplastik malzemelerin eritilerek üç boyutlu (3B) yazıcılar yardımıyla kat kat biriktirilmesi sureti ile hızlı ve kolay bir üretim imkanı sağlamaktadır. Bu üretim karmaşık şekilli nesnelerin üretimine imkan sağlamakta ve sonrasında malzemenin fazladan bir işleme gerek duymadan kullanıma hazır hale getirmektedir. Ayrıca geleneksel üretim yöntemleri ile kıyaslandığında üretim maliyetinin düşük olması en önemli yararlarından birisi olarak gösterilmektedir. 3B yazıcılarda kullanılacak polimerlerin kat kat biriktirmeye imkan sağlaması için belirli bir vizkozite değerine sahip olması gerekmektedir. Bu sebeple, düşük viskozitedeki polilaktik asit (PLA), akrilonitril bütadiyen stiren (ABS) gibi malzemeler kullanılmaktadır. Fakat, bu malzemelerin mekanik dayanımlarının yüksek olmaması kullanım alanlarını havacılık, savunma ve uzay gibi mekanik isterleri yüksek endüstrilerde kısıtlamaktadır. Bu endüstriler için ise yüksek performanslı polimerlerin (polieterimid (PEI) ve polieter eterketon (PEEK)) kullanımı ön plana çıkmaktadır. Bu malzemeler, beklenen mekanik isterleri karşılarken yüksek operasyon sıcaklıklarında kullanılabilirliğe sahip oldukları için avantajlıdırlar.

Polimer malzemeler düşük yoğunlukları, yüksek korozyon dirençleri, düşük üretim maliyetleri gibi özellikleri sebebiyle termal yönetim uygulamaları için güçlü bir alternatif olarak görülmektedir. Fakat polimer malzemelerin düşük termal iletkenlikleri bu alanda kullanımlarını kısıtlamaktadır. Bu engel polimer malzemelere çeşitli katkılar yaparak polimer matrisli kompozit üretimi ile aşılmaya çalışılmaktadır. Bu katkı malzemeleri temel olarak üç farklı türde bulunmaktadır, bunlar: (i) Seramik-bazlı katkılar, (ii) Metal-bazlı katkılar, ve (iii) Karbon-bazlı katkılardır. Polimer matrisli kompozit üretimi sırasında etkili bir termal iletkenlik değerine ulaşılabilmesi için, katkı

malzemesinin uygun boyutlarda seçilmesi ve bu malzemelerin matris içerisinde etkili bir şekilde dağıtılması gereklidir.

Bu tez, havacılık, uzay ve savunma alanlarında kullanılmak üzere termal yönetim uygulamaları için, 3B yazıcı yöntemi ile üretimi gerçekleştirilecek filaman geliştirilmesini hedeflemektedir. Bu kapsamda, PEI 3B yazıcılarda üretime uygun olması, yüksek mekanik özellikleri ve yüksek operasyon sıcaklığı dolayısı ile polimer matris olarak seçilmiştir. Bu polimer malzeme, seramik-bazlı bir katkı olan hegzagonal bor nitrür (h-BN) ve karbon-bazlı bir katkı olan karbon nanotüp (CNT) malzemeleri ile güçlendirilmiş ve termal iletkenlik değerlerinin yükseltilmesi hedeflenmiştir.

Üretimler sırasında ilk olarak ekstrüder üretimi için bir optimizasyon çalışması yürütülmüş ve katkı malzemelerinin polimer matris içerisinde etkili bir şekilde dağıtılmasına çalışılmıştır. Optimizasyon çalışmaları sırasında ekstrüder vidasının dönme hızı, ekstrüder çalışma sıcaklığı ve malzemelerin besleme oranını belirlemek amacıyla, kütlece %20 BN katkılı PEI kompozitler farklı çark hızlarında (50-310 rpm), belirlenen sıcaklıklarda (350-380 °C) ve seçilmiş olan besleme oranlarında (0,5-1,5 kg/s) üretilmiştir. Katkı malzemelerinin polimer içerisindeki etkin dağılımını tespit etmek amacı ile reoloji analizleri yapılmıştır. Reoloji ölçümleri sırasında frekans tarama testleri uygulanmış ve düşük frekans oranlarında malzemenin davranışı incelenmiştir. Reoloji ölçümleri neticesinde en iyi dağılımlara 250 rpm çark hızı, 360 °C çıkış sıcaklığı ve 1 kg/s besleme oranında ulaşıldığı görülmüştür. Ayrıca, reoloji ölçümleri neticesinde en iyi çalışma koşulu olarak belirlenen parametrelerin termal iletkenlik üzerine etkisi incelenmiştir. Bu amaçla farklı çalışma koşulları ile üretilen kompozit malzemelerin termal iletkenlik ölçümleri alınmıştır. Bu sonuçlara göre, termal iletkenlik değerlerinin, her bir parametre için $\approx$ %6 artış gösterdiği tespit edilmiştir.

Kompozit malzeme üretimleri bu şartlara göre gerçekleştirilerek çift vidalı ekstrüder yardımı ile PEI sırası ile kütlece % 5, 10, 15, 20, 25 ve 30 BN ile katkılandırılarak BN/PEI kompozit filamanları ve granülleri üretilmiştir. İkinci bir aşama olarak ise kütlece % 1, 2, 3 ve 5 CNT yardımı ile hibrit kompozit filamanları ve granülleri BN ve CNT arasındaki sinerjik etkileşiminden faydalanmak amacı ile kullanılmıştır. Sonrasında, filamanlar 3B yazıcı kullanılarak, granüller ise sıcak-basınç tekniği ile şekilllendirilerek termal iletkenlik ölçümlerine uygun numuneler üretilmiştir.

Kompozit malzeme üretimi sonrasında termogravimetrik analiz (TGA), diferansiyel taramalı kalorimetre (DSC) testleri uygulanarak katkı malzemelerinin, oranlarının bozunma sıcaklığı ve camsı geçiş sıcaklıkları üzerine etkisi incelenmiştir. TGA ve DSC ölçümleri sonucunda BN katkısının malzemenin bozunma ve camsı geçiş sıcaklıklarını değiştirmediği, CNT katkısının ise malzemenin bozunma sıcaklığını yaklaşık 20 °C yükselttiği, camsı geçiş sıcaklığını ise değiştirmediği görülmüştür. Ardından yapılan reoloji testleri neticesinde katkı malzemelerinin viskozite üzerine etkileri incelenmiştir. BN/PEI kompozitleri için reolojik sızıntı eşiğinin kütlece %15 BN, CNT/BN/PEI kompozitleri için ise sızıntı eşiğinin kütlece %1 CNT olduğu görülmüştür. Son olarak kompozit malzemelerinin termal iletkenlik ölçümleri gerçekleştirilmiş ve kütlece %30 BN katkısı ile katkısız PEI malzemesinin termal iletkenlik değerinin 0.21 W/m K'den %289 artış ile 0.82 W/m K değerine yükselmiştir. Benzer bir artış hibrit kompozit üretiminde daha düşük katkı oranında elde edilmiştir. Kütlece %15 BN barındıran CNT/BN/PEI kompozitlerinin termal iletkenliği kütlece %5 CNT katkısı ile katkısız PEI ile kıyaslandığında %287 artarak, 0.81 W/mK

değerine ulaşmıştır. Bu iki değer kıyaslandığında hibridizasyon yöntemi kullanılarak daha düşük katkı oranlarında aynı değerin elde edilebildiği görülmüştür.

Sonuç olarak, bu tez çalışması kapsamında PEI malzemesinin termal iletkenlik ve akış özelliklerine BN ve CNT etkisi incelenerek 3B basılabilir, termal iletken polimer kompozit filamanların üretimi gerçekleştirilmiştir.

1. INTRODUCTION

Thermal dissipation has become a critical problem in recent years due to the appearance of new devices and the functionalization of electronic devices [1]. To meet the demand of high heat capacity materials in new emerging technologies and overcome the issues of conventional materials, such as high thermal expansion coefficients, low corrosion resistance, and high production cost, development of novel polymer composite materials with enhanced thermal conductivities is needed. Rather than conventional metals (having thermal conductivity over 70 W/m K [2]), polymers can be an alternative for next-generation heat exchangers in which lightweight and corrosion resistance is crucial. However, substantial challenges may arise for several thermoplastics with their low mechanical strength, physical aging, low service temperature, and processability. Hence, novel polymer composites reinforced with fillers with high thermal conductivity and mechanical strength may be an alternative solution for next-generation heat exchangers with a careful approach in design and manufacturing [3]. Therefore, thermal management systems have become mandatory to dissipate the generated heat. In a thermal management system, besides high thermal conductivity low thermal expansion coefficient (CTE) is also required for dimensional stability of electronic devices.

Polymer matrix composites (PMCs) with their lightweight, corrosion resistance, cost efficiency, low thermal expansion coefficients, and tunable mechanical and thermal properties offer an alternative solution for next-generation heat exchangers when a careful approach in design and manufacturing is performed [3]. On the other hand, compared to metals, commodity polymers exhibit considerably lower thermal conductivities. To evaluate the potential of thermoplastics as lightweight solutions to existing metallic heat exchangers a rigorous addressing should be performed to establish the phonon transport mechanisms [4]. The thermal conductivity of PMCs can be influenced by many factors such as filler type, dispersion of fillers, size of filler, and processing conditions. The efficient factors should be understood thoroughly

and optimized to improve the thermal conductivity of composites. Therefore, incorporating nano- or micro-fillers to high-performance polymers and dispersing them in a polymer matrix can help overcome challenges arisen from low thermal conductivity of thermoplastics with a minimal weight penalty.

Multifunctional nanocomposites by three-dimensional (3D) printing is a novel technology for a new class of materials that hold the potential combinations of properties from both micro- and nano-fillers such as carbon nanotubes (CNTs), and hexagonal boron nitride (h-BN). Consistency, cost, and reliability in volume production, which are widely related to processing techniques, are limitations for the production of nanocomposites, and these can be solved by additive manufacturing (AM). In AM, precise control and tailoring of nanocomposites are applicable and micro- or nano-fillers hosted by polymer matrices manufactured in 3D printing can offer significant advantages such as customized geometries, lightweight cellular architectures, single tool manufacturing, and easy integration of several parts with multi-functionality with multi-material possibilities. Among several AM technologies, Fused Deposition Modelling (FFF) is a more viable method to achieve thermally conductive cellular nanocomposites either by structural or non-structural applications within its ease to build-use and high manufacturing resolution than others [5]. The key point here is to fabricate micro- or nano-reinforced thermoplastic as the monofilament spool of a 3D printer.

Production and use of reinforced thermoplastic filaments which have enhanced mechanical properties and thermal conductivity are the main subjects of this thesis. More specifically, these reinforced thermoplastic filaments are intended to be used in thermal management applications. To fabricate these multifunctional filaments which could be used in 3D printers, Polyetherimide (PEI), a high-performance thermoplastic, is studied for reinforcement with micro-BN and nano-CNT fillers with a hybrid approach that can provide the composites with the adequate thermal conductivity.

1.1 Literature Review

1.1.1 Polymer composites for next generation thermal management applications

PMCs with their lightweight, corrosion resistance, cost efficiency, and tunable mechanical and thermal properties offer an alternative solution for next-generation thermal interface materials and heat exchangers. However, compared to metals, commodity polymers have thermal conductivities very lower than metals. To evaluate the potential of thermoplastics as lightweight solutions to existing applications, phonon transport mechanisms should establish precisely.

The main goal of the thermal management applications is to keep cool of electronic devices by dissipating the heat. First, to keep cool of electronic devices the interface between the heat source and heat sink needs to be used carefully. Thermal conduction between the heat source and the heat sink can be improved by thermal interface materials (TIMs). When the contact area is decreased, the air in the environment begins to fill the gaps in the contact area. Then, heat flow decreases throughout the interface because of the low thermal conductivity of air. Therefore, the contact area between the heat source and the heat sink should be increased as much as possible [6]. The importance of thermal interface materials is shown in Figure 1.1. The TIMs should meet the needs such as high thermal conductivity, minimal thickness, high impermeability and non-toxicity of industry [7].

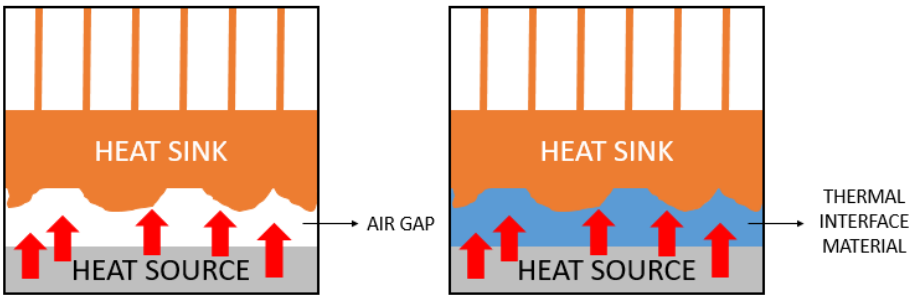

Figure 1.1 : TIMs applied to fill the air gap.

The other fundamental component of the thermal management systems is heat exchangers which enable to transfer heat without mixing two different fluids. The conventional heat exchangers have been fabricated using metals such as stainless

steel, copper and aluminum. Rather than metals offering high thermal conductivity, production cost and heaviness are the major problems of them. Besides, a surface treatment process needs to be applied, if the working fluids are corrosive [8]. As a result, polymer heat exchangers are of interest in recent years by many researchers. The first polymer heat exchanger was introduced by DuPont in 1965 [9] and they have a wide area of use such as water desalination systems, solar water heating systems, air-conditioning, space applications, and chemical and petrochemical processing as presented in Figure 1.2 [4, 10].

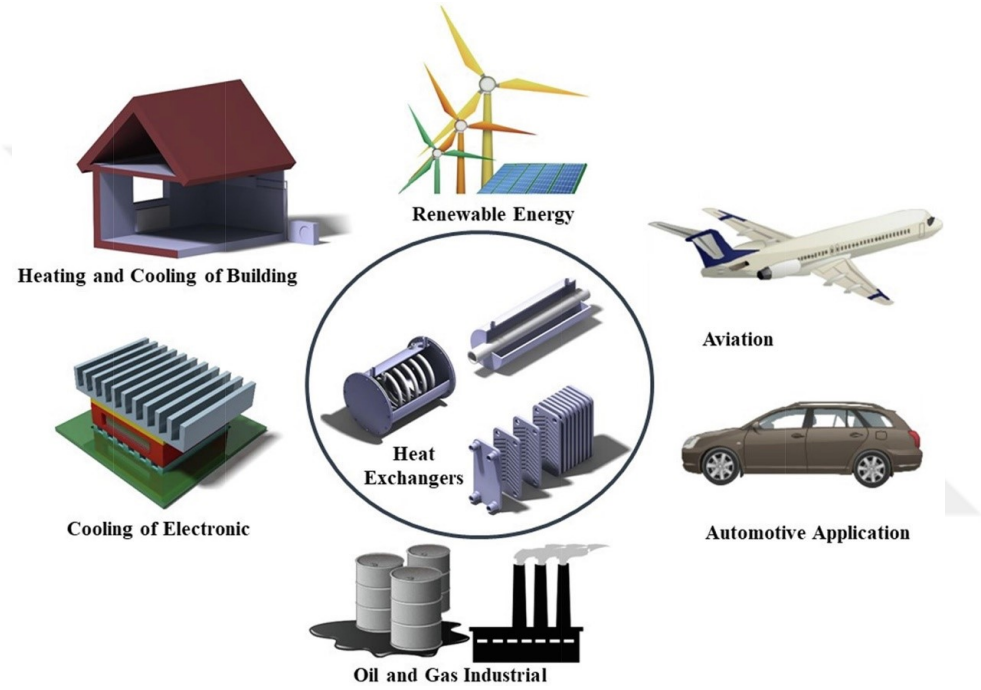

Figure 1.2 : Uses of heat exchanger in various devices [10].

The heat exchangers can be classified according to their shapes and physics as shown in Figure 1.3. The suitable heat exchanger type should be determined by work environment and a careful design process should be performed.

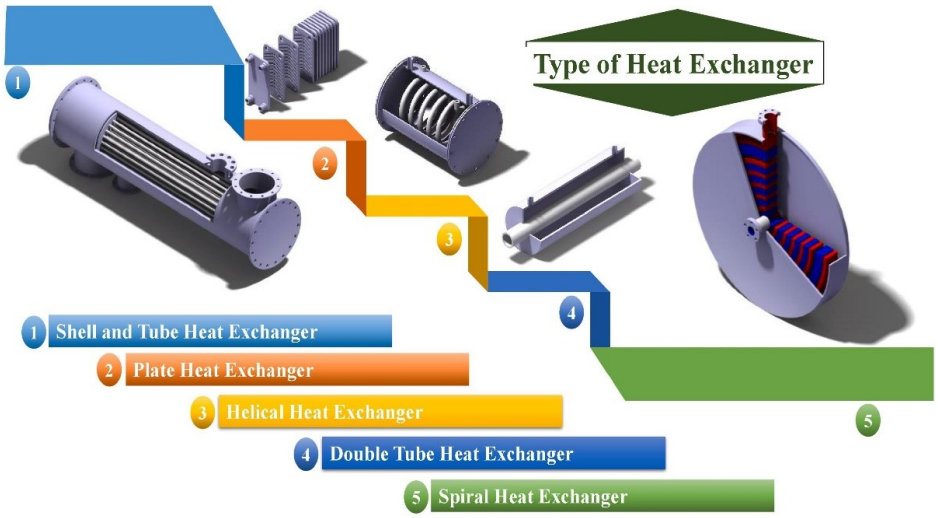

Figure 1.3 : Common heat exchanger types [10].

1.1.2 High performance thermoplastic polymer composites with potential use in additive manufacturing

AM which is also known as three-dimensional (3D) printing or rapid prototyping (RP), is a novel technology for fabrication of the objects that may come in complex shapes. This method enables the fabrication of complex objects from the 3D model guided with computer-aided design (CAD) by usually adding materials layer by layer [11]. After the design, a 3D model with CAD software, Surface Tessellation Language (STL) file is created to transfer the designed model to the 3D printer as a geometric code file (g-code). Several printing techniques such as FFF, selective laser sintering (SLS), inkjet 3D printing (3DP), stereolithography (SLA) and 3D plotting have been used to fabricate 3D objects [12]. Schematic representations of 3D printing techniques are shown in Figure 1.4. Several printing techniques have been used to fabricate 3D objects. These printing techniques have advantages and drawbacks in the fabrication of objects. Therefore, the starting material, processing speed, cost, and performance should be determined in order to choose a suitable technique [12].

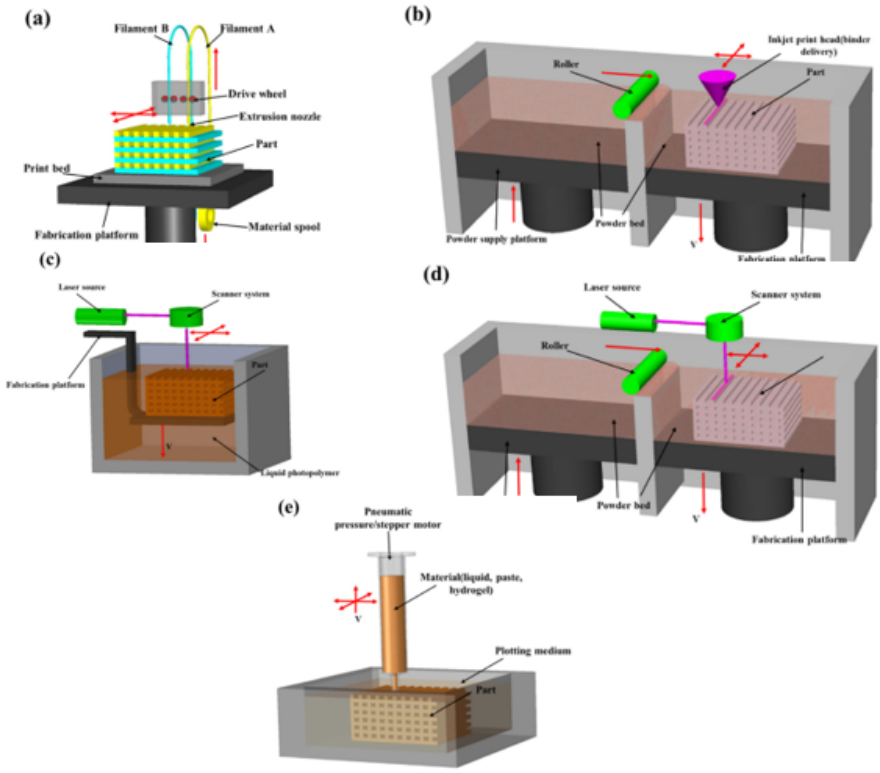

Figure 1.4 : Widely used 3D printing techniques a) FFF, b) 3DP, c) SLA, d) SLS, e) 3D plotting [12].

FFF technique is one of the most widely used techniques to fabricate polymer composites thanks to advantages such as cost efficiency, high speed, and simplicity. Thermoplastic polymers such as polylactic acid (PLA), acrylonitrile butadiene styrene (ABS), PC, PEI, PEEK, and PPS are commonly used as feedstock materials in the FFF technique. The production of 3D products is completed by melting the polymers in the nozzle and depositing their layers on each other [12]. The quality of the final product mainly depends on the processing parameters such as layer thickness, raster width, raster angle and air gap [13]. FFF technique suffers from mainly two difficulties which are limited feedstock materials requiring suitable viscosity and the need to have the feedstock in filament form [12]. Therefore, suitable polymers should be fabricated for their use in the FFF. The fabrication of thermally conductive filaments for the FFF has been studied by various researchers. Hwang et al. fabricated thermally conductive Cu/ABS filaments and investigated the effect of Cu content on different parameters. They achieved 41% increase in thermal conductivity of ABS with the addition of 50 wt.% copper and reached 0.912 W/m K. However, the results showed that the increasing copper content led to a decrease in tensile strength and tensile strain as shown in Figure 1.5 [14]. In another study, Liu et al. investigated the behavior

of thermal conductivity and CTE of BN/TPU polymer composites along with two directions: printing direction (PD) and thickness direction (TD) [15]. The BN/TPU polymer composites were fabricated with different BN fractions by an internal mixer and twin-screw extruder processes, respectively. The CTE values in the PD decrease with the increasing BN loading with negative CTE value of BN fillers along the in-lane direction. However, CTE values in the TD increased with the increasing BN concentration because of the high CTE value of BN filler along the out-line direction as shown in Figure 1.6(a). The thermal conductivity behavior of BN/TPU composites differs based on whether printing or thickness directions are considered. Even though the thermal conductivity of the composites increased with the addition of BN in the TPU matrix, the increase in thermal conductivity in the PD was higher than that of in the TD as presented in Fig. 1.6((b).

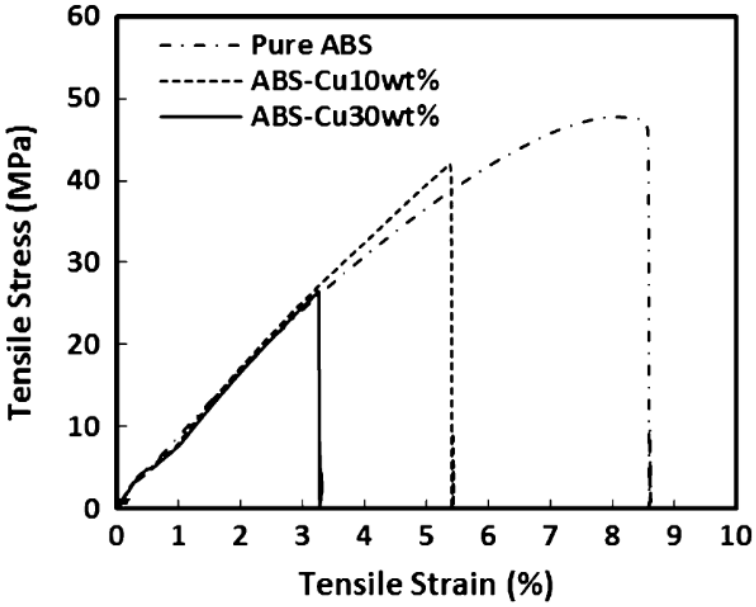

Figure 1.5 : Stress-strain curve of Cu/ABS composites [14].

To assess the hybridization effect on the thermal conductivity, Lebedev et al. fabricated PLA matrix composite filaments reinforced with SWCNTs and graphite (G) for the FFF by the melt-compounding method [16]. Thermal conductivity of PLA improved by more than 14 times and reached 2.73 W/m K from 0.193 W/m K with the incorporation of 30 wt.% G. Following these promising results, hybrid CNTs/G/PLA composites were fabricated. Thermal conductivity of the 1 wt.% CNTs/30 wt.% G/PLA composite was improved by approximately 40% and reached 3.8 W/m K (Fig. 1.7).

1.1.3 Strategies to enhance thermal conductivity of polymers

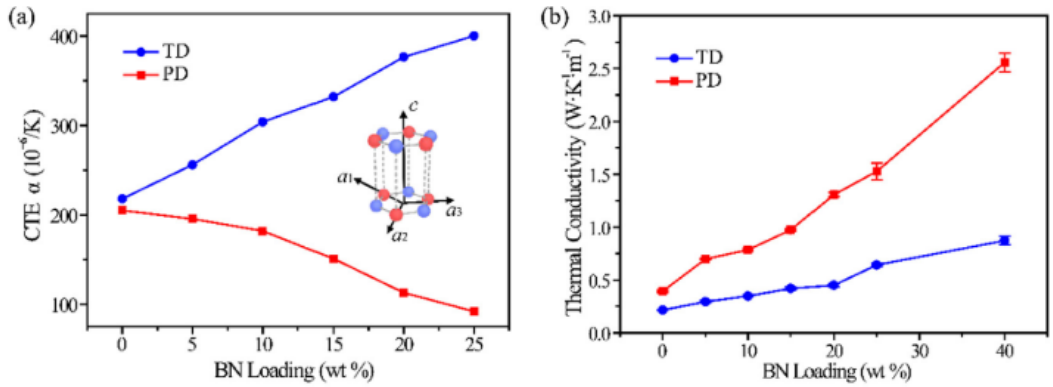

Figure 1.6 : (a) CTE and (b) thermal conductivity of BN/TPU composites with different BN loadings [15].

Heat can be transported by electrons and holes or phonons in materials. While electrons and holes are main responsible for heat carrying in metals, heat is carried by phonons [17]. The phonon can be described as quantized energy of lattice vibration [18, 19]. A graphical presentation of phonon has shown in Figure 1.8. The heat carrying phonon can be scattered due to imperfections in a polymer matrix [20]. The low thermal conductivity of polymers arises from phonon scattering. There are three main phonon scattering mechanisms such as phonon-phonon scattering, phonon-impurity scattering, and phonon-boundary scattering as shown in Figure 1.9. If two different phonons collide with each other during their movements, they scatter with reducing each other's energies. This situation called as phonon-phonon scattering.

Furthermore, the phonons may encounter with imperfections such as impurities in a matrix. The impurities can change the lattice direction and momentum can block phonon transport and a small amount of impurity may lead to a tremendous decrease in thermal conductivity [21].

The last scattering mechanism can be described as an encounter of phonons with boundaries. After a phonon approach a boundary, it scatters and thermal transport is hindered [19]. Therefore, phonons should move easily throughout the polymer matrix in order to achieve high thermal conductivity in polymers. The potential approaches to make phonon transport easier will be discussed further.

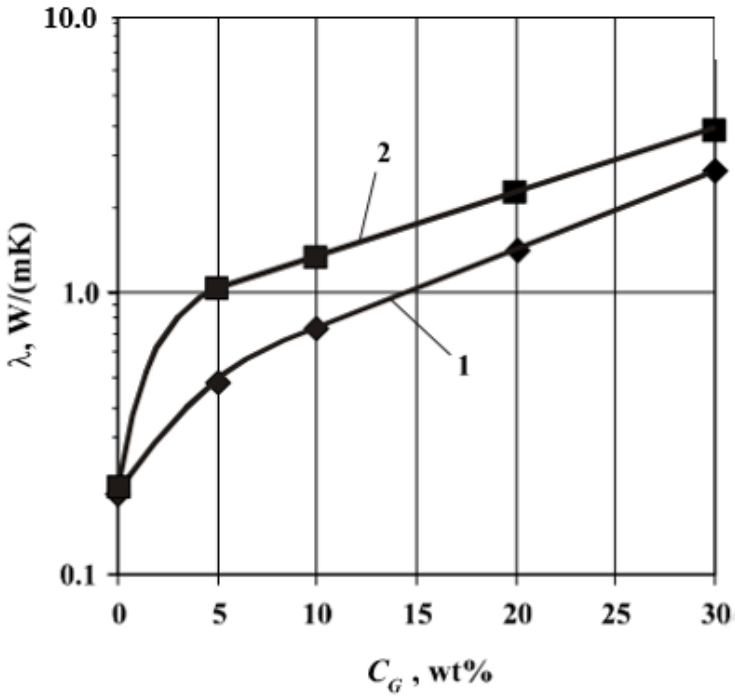

Figure 1.7 : Thermal conductivity as a function of the graphite content: 1, without CNTs: 2, with 1 wt.% CNTs [16].

Head: particle nature of phonon
Tail: wave nature of phonon

Figure 1.8 : Presentation of phonon [19].

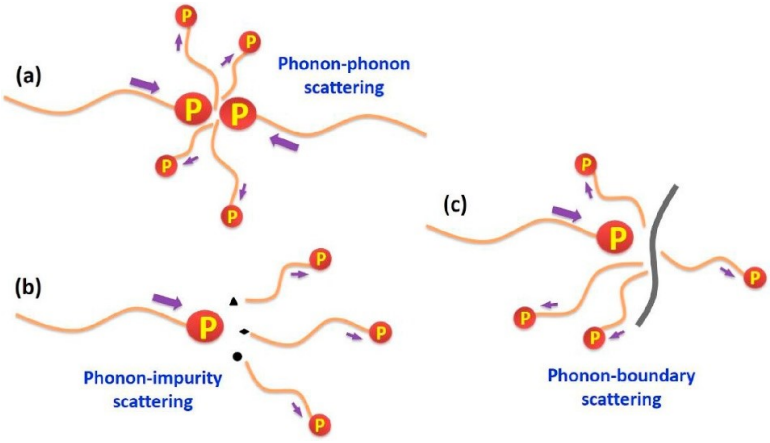

Figure 1.9 : Phonon scattering mechanisms a) phonon-phonon scattering, b) phonon-impurity scattering, c) phonon-boundary scattering [19].

1.1.3.1 Common filler types used in polymer reinforcement

Thermal management applications require high thermal conductivity values and the required thermal conductivity can be adjusted depending on the applications. Polymer-based heat exchanger fabrication has been carried out in several fields such as air conditioning and heat recovery. However, it seems difficult for polymer materials to replace metals in thermal management applications due to their low thermal conductivity [22–24]. To achieve high thermal conductivity in polymeric structures, various types of fillers such as metals, ceramics, and carbon-based materials are used [2].

Metallic fillers including copper (Cu), silver, aluminum, gold, and nickel have been used for thermally conductive polymer composite fabrication for many polymer matrices such as polycarbonate (PC) [25], polyethylene (PE) [26], polypropylene (PP) [27], and epoxy [28] resins. Polymer composites involving metallic fillers show high thermal conductivity and high electrical conductivity. However, high density and low corrosion resistance of metallic fillers are important problems and these fillers cannot be used in applications that require lightweight and corrosion resistance features. The thermal conductivity of the composites mainly depends on the thermal conductivity and the volume fraction of the fillers [4]. Thermal conductivity, coefficient of thermal expansion, and density of some of the widely used metal fillers are given in Table 1.1.

Table 1.1 : Thermal conductivities of metallic fillers [17, 29].

Material	Thermal Conductivity (W/m K)	CTE (10^{-6} / °C)	Density (g/cm^3)
Aluminum	247	23	2.7
Copper	483	17	8.9
Nickel	158	13	8.9
Silver	450	18	10.49

Carbon-based fillers such as carbon fiber, carbon black, graphene, graphite, and CNTs improve the thermal and electrical conductivity and mechanical properties of the composites [30–32]. Furthermore, low thermal expansion coefficients and high corrosion resistance of carbon-based fillers make them suitable for PMCs.

One-dimensional (1-D) CNTs and two-dimensional (2-D) graphene nanoplatelets (GNP) have been widely used as thermally conductive fillers. Single-walled carbon nanotubes (SWCNTs) and multi-walled carbon nanotubes (MWCNTs) are the most promising materials for polymer composites having high intrinsic thermal conductivity as high as 3000 W/m K [33]; however, it is difficult to disperse them in a matrix and they suffer from high production cost. On the other hand, GNP is another widely studied filler because of its high thermal conductivity and easier dispersion compared to CNTs in a polymer matrix with its 2-D geometry. Considering the ease of dispersion while still attaining high thermal conductivity, GNP has been acknowledged for its better potential for increasing the thermal conductivity of polymer matrices [34]. The thermal conductivities of some of the carbon-based fillers are given in Table 1.2.

Table 1.2 : Thermal conductivity of carbon-based fillers [35, 36].

Material	Thermal Conductivity (W/m K)
Carbon fiber	530-1100
Carbon black	6-174
Graphene	5000-6000
Graphite	100-400
Carbon nanotubes	2000-6000

Ceramic-based fillers such as aluminum nitride (AlN), BN, silicon carbide (SiC), and beryllium oxide (BeO) have been widely used for thermal management applications especially when the application product requires high thermal conductivity and low electrical conductivity [37]. The thermal conductivities of the most commonly used ceramic-fillers can be seen in Table 1.3. High thermal stability and low thermal expansion coefficient of ceramic fillers can be used to introduce high thermal stability and dimensional stability to polymer composites [4]. Leung et al. investigated the thermal conductivity of polyphenylene sulfide (PPS) composites by BN. The thermal conductivity of BN/PPS composite increased with increasing h-BN fraction, particularly showing an increase of 800% with the addition of 33.3 vol.% h-BN [38]. Wu et al. achieved a 300% improvement in the thermal conductivity by adding 57.4 vol.% AlN compared with neat PEI. Additional results include 27% improvement in the tensile strength with the addition of 12.6 vol.% AlN [39].

Table 1.3 : Thermal conductivity of ceramic-based fillers [4, 29].

Material	Thermal Conductivity (W/m K)	CTE (10^{-6} / °C)	Density (g/cm^3)
Aluminum nitride	320	4.5	3.3
Boron nitride	260	6	3
Silicon carbide	270	3.7	3.3
Beryllium oxide	260	6	3

1.1.3.2 Effect of hybridization

The hybridization effect can be described as a combination of two or more different fillers to achieve even greater thermal conductivity [19]. To date, various polymers such as high-density polyethylene (HDPE), PP, PPS, PEI, and polyether ether ketone (PEEK) have been used for thermally conductive composite production [39–43]. Che et al. investigated the hybridization effect on the thermal conductivity using BN and CNT fillers incorporated into the HDPE matrix. The study showed that using fillers in different sizes and types has an enormous effect on thermal conductivity. Using 25 wt.% BN and 3 wt.% CNTs led to 300% increase in thermal conductivity. However, desirable thermal conductivity values could not be achieved with filler concentrations mentioned above. This nonlinear thermal conductivity behavior arises from the inability of thermal conductivity pathway formation [40]. In another study by Wu et al., the PEI matrix was filled with CNTs and AlN. Their results showed that the thermal conductivity of the composite increased substantially by 670%, reaching 1.62 W/m K when the filler loading was 80 wt.% AlN and 5 wt.% CNTs [39].

The thermal conductivity of polymer composites mainly depends on the intrinsic thermal conductivity and state of dispersion of fillers as mentioned before. Another important point is; the size of filler which affects the thermal conductivity of the composite. The interface between polymer matrix and filler has an important role in the thermal conductivity of PMCs and the main reason for not achieving the desired thermal conductivity in PMCs is interfacial resistance between polymer matrix and filler. The matrix-filler interface can vary depending on the filler size. In this context, various studies have been conducted in the literature to understand the size effect of the filler [44–46]. Tung-Lin Li investigated the filler size effect using different sizes of BN (micro- to nano-sized BN fillers) for Polyimide (PI)/BN composite fabrication. The

results showed that the incorporation of micro-size BN in PI matrix displayed about 25% higher thermal conductivity than nano-size filler addition [45]. This behavior was explained by interfacial thermal resistance. The thermal conductivity of composite can be improved by using a small size of a particle because using small particles reduces the thermal resistance by reducing contact points between matrix and filler [27, 47].

1.1.3.3 Dispersion quality and process parameters

The thermal conductivity of polymer composites is dominated by phonon scattering mechanisms in the polymer matrix [48]. Burger et al. stated that the phonon scattering mechanism is related to the state of dispersion, filler/matrix interfaces, and filler alignment and networking [48]. The effect of dispersion was studied in the literature by various researchers [48–50]. To assess the dispersion effect on the thermal conductivity, Karippal et al. fabricated two different specimen sets for 8 vol.% CNT/epoxy composites using a twin-screw extruder. In the first set, CNTs were dispersed in acetone with ultrasonication before extrusion while the CNTs in the second set were directly dispersed during extrusion. The results revealed that 60% and 25% increases in the thermal conductivity values were achieved with the first and second sets, respectively. In another study, researchers investigated two different cases with several weight fractions of CNT/epoxy nanocomposites: one with well-dispersed CNTs and another with poorly dispersed CNTs. Thermal conductivity values were increasing with enhanced dispersion quality. Specifically for 1.5 wt.% CNT/epoxy composite specimens, the thermal conductivity of the well-dispersed and the poorly-dispersed cases were different by 33% [50]. On the other hand, Burger et al. investigated the relationship between thermal conductivity and dispersion by manufacturing three different 5 wt.% CNF/epoxy composites with different dispersion qualities. The results showed that well-dispersed fillers led to a decrease in thermal conductivity with an unexpected trend and the thermal conductivity values were increased with the poorly dispersed CNFs into epoxy by 26%. When the dispersion quality was increased slightly, the enhancement in the thermal conductivity reduced to 13%. Finally, it was observed that when the dispersion quality was improved even further, the increase in the thermal conductivity values remained at 17%. Based on the information above, high dispersion quality may not be quite significant to achieve higher thermal conductivity. Therefore, additional studies should be performed

in order to completely understand the effect of dispersion state on the thermal conductivity coupled with the phonon transport mechanism.

The thermal conductivity of composites was also affected by the process parameters. Processing techniques such as solution mixing and melt mixing/compounding have a great influence on the thermal conductivity [19, 51, 52]. Therefore, the determination of optimum process methods and conditions should be carried out to achieve greater thermal conductivity. The melt mixing techniques such as extruders and internal mixers have been used to fabricate thermally conductive PMCs [53–55]. The melt compounding process can be determined as an outstanding process for industrial applications among all processing techniques due to cost efficiency and direct process. Another advantage of the melt compounding is the possibility of mass production without using any solvent during the process. However, applying high shear forces during the melt mixing process leads to decreases filler aspect ratio. Therefore, even though the melt mixing process can be nominated to be the best way for industrial production, it imposes a limit on the thermal conductivity of PMCs [56]. The second most used technique is the solution mixing process which allows for homogeneous dispersion of fillers in a polymer solution [57]. Effect of sonication conditions on thermal conductivity and its improvement has been investigated by several researchers [39, 58–61]. The researchers showed that sonication bath and power of sonication have a great influence on the dispersion of fillers. Therefore, the effective process parameters should be optimized in order to achieve well dispersion.

Although, the dispersion of CNTs in a polymer matrix is difficult using a melt mixing technique, it possible to achieve dispersion by the solution mixing technique [61]. However, the solution mixing technique is not preferred by industrial applications because it has limitations for a mass production [48].

1.1.4 Summary

The fabrication of thermally conductive polymer composite for thermal management applications is an attractive topic for the industry. Many studies have been carried out to understand thermal conduction transport and how thermal conductivity can be increased in polymers. Each of these topics were discussed in here including: thermal management applications, thermal conductivity mechanism, and main parameters

to fabricate thermally conductive polymer composites. This thesis discusses the importance of material selection, process selection, and process parameters for multifunctional filament manufacturing with carbon and ceramic based fillers as a hybrid approach for 3D printing. The relation between the processing parameters and thermal conductivity is established widely. The well dispersion of fillers in the polymer matrix was also proposed to be a method to improve thermal conductivity. Besides, the hybridization technique was suggested to create a synergistic effect.

1.2 Motivation

A high heat transfer rate with minimum thermal expansion at the operating temperature is one of the most critical requirements that a heat exchanger should satisfy. Hence, many metallic thermal management systems are designed and built for several applications. Rather than conventional metals, polymers can be an alternative for next-generation heat exchangers in which weight and corrosion resistance are critical. Besides, novel polymer composites having high thermal conductivity and high operating temperatures are promising solutions with an ease of manufacture.

As an effective method of AM, FFF is a novel technology enabling the production of complex structures through cost-effective and easy processes. To achieve the full potential of the micro- and/or nano-fillers in nanocomposites, beyond processing conditions, precise control in production is crucial. AM, 3D printing technology, offers a powerful toolbox in routine production steps of AM and provide additional benefits for advanced applications with complex geometries and material tailoring [4].

In this study, PEI was selected as the polymer material with its high mechanical properties, high service temperature and high resistance to corrosion. MWCNTs and h-BN were selected as fillers having high thermal conductivity. In this scope, BN/PEI polymer composites and CNTs/BN/PEI hybrid polymer nanocomposites were fabricated in a custom-built melt extruder system as a feedstock filament for FFF to develop nanocomposite filaments with thermal conductivity over 1 W/m K. After determining the optimum processing conditions, thermal conductivity properties and printability of the polymer composites filaments were investigated.

1.3 Thesis Overview

This study is reported in four chapters. A background and literature review is presented in Chapter 2 on the following topics: mechanism of thermal conductivity in polymers, thermally conductive filler types, the influence of hybridization, influence of filler dispersion, influence of filler size, influence of the process on thermal conductivity, thermal conductivity measurement techniques, additive manufacturing method, and summary. Chapter 3 presents the study on the fabrication and characterization of polymer composites, detailing parametric studies conducted in this research. Furthermore, the effect of filler on the thermal properties, rheological properties, microstructure, and thermal conductivity are presented in Chapter 3. Finally, the thesis concludes with an overview of this research and future recommendations.

2. MATERIALS AND METHODS

Developing advanced thermal management materials from polymers require creative solutions to achieve enhanced thermal conductivities for next-generation electronic packaging. Hence, in this work a high-performance polymer reinforced with micro and nano-sized filler was discussed with critical parameters of processing. The melt mixing process was employed by a custom-built extruder to achieve the optimal filler concentrations and processing parameters. A parametric study has been conducted to optimize the rotor speed, temperature, and feeding rate conditions for achieving high quality dispersion state of BN fillers in an amorphous high-performance polymer chain, such as PEI, and proper chain alignment of the aforementioned polymer is studied. Additionally, hybridization is also investigated to promote the idea of creating enhanced conductive pathways through various sized and shaped fillers and avoid phonon scattering [19, 62]. Finally, an optimal h-BN and CNTs ratio is being explored as hybridization effort to develop high thermal conductivity polymer composites. An amorphous thermoplastic polymer – (i) PEI and two types of thermally conductive fillers – (i) h-BN, and (ii) MWCNTs were selected as matrix and reinforcements respectively for fabricating the polymer composites using a melt compounding technique with a custom-built twin-screw extrusion. After melt compounding process, fabricated composite granules were either. hot pressed and 3D printed in a cylindirical disc form with appropriate dimensions for thermal conductivity measurement.

2.1 Matrix: Polyetherimide

High performance polymers were used to improve mechanical properties of the composites. Moreover, high service temperature and ease on 3D printing became the main selection criteria for thermal management applications. In this context, high-performance polymers such as PEI, PEEK, PPS may be a suitable choice because of their high mechanical strength, good thermal stability, and high service temperature. Among these high performance thermoplastics, PEI has an amorphous microstructure

while PEEK and PPS are semi-crystalline. The microstructure of a polymer has an important effect on thermal conductivity because of chain alignment, orientation and density, melt and glass transition temperature variations and operation temperatures in these polymers can bring differences. To date many researchers investigated the thermal conductivity differences between amorphous and semi-crystalline polymers. When semi-crystalline polymers were considered within their well-oriented chain configuration, thermal conductivities of them were higher than amorphous polymers that cause phonon scattering [63–65]. Nevertheless, most of the studies reported in the literature have focused on investigating thermal conductivity difference between neat polymers rather than of the composites of them reinforced with fillers. Therefore, a novel approach to reinforce PEI polymer with several filler/loading rates were investigated in here. PEI pellets were purchased from Sabic (Ultem 1010) as a matrix material with a density of 1.27 g/cm^3, and *Tg* 217 °C.

2.2 Filler Materials

2.2.1 Hexagonal boron nitride

h-BN has planar sheets crystal structure which covalently bonded boron and nitrogen atoms [66] and Van der Waals forces hold together of different layers. h-BN has different thermal conductivity based on the direction due to its anisotropic crystal structure. The in-plane thermal conductivity of h-BN has been estimated to changes 100-400 W/ m K, while the through-plane thermal conductivity is around 3 W/m K. Besides, h-BN was chosen due to its high thermal conductivity and lubricant property enabling higher amount of filler addition during the melt compounding process [67]. The filler properties are given in Table 2.1

2.2.2 Multiwalled carbon nanotubes

CNTs have attracted great attention in recent years due to their extraordinary electrical and thermal properties [68]. Thermal conductivity of individual CNT may reach up to 3000 W/ mK at room temperature. CNTs are used as reinforcement to increase polymer thermal conductivity. However, the estimated effect is not high as expected due to curved structure of CNT, impurities and structural defects [17, 69].

Table 2.1 : Properties of h-BN, and CNTs.

Filler Name	Thermal Conductivity (W/m K)	CTE (10^{-6} / °C)	Density (g/cm^3)	Size (m)	Purity (min) %
h-BN*	100-400	-5.65	2.25-2.35	4-10	99.5
CNTs**	2000 (theoretical)	1.8	Negligible	5-15	90

* Civelek Porselen Data Sheet
** Nanokomp Data Sheet

2.3 Fabrication of Polymer Composites

The BN/PEI and CNTs/BN/PEI composite granules and filaments were fabricated by twin-screw extrusion and single-screw extrusion processes, respectively. In here, a custom-made twin-screw extruder were employed for all mixing processes designed by Kökbir Import&Export (Figure 2.1). A detailed technical information table for screws and technical specifications are listed in Table 2.2.

Both of the melt-processed composite granules and filaments were then used to fabricate the specimens for thermal conductivity measurements using a hot press and 3D printer, respectively. The schematics presenting the experimental route is given in Figure 2.2.

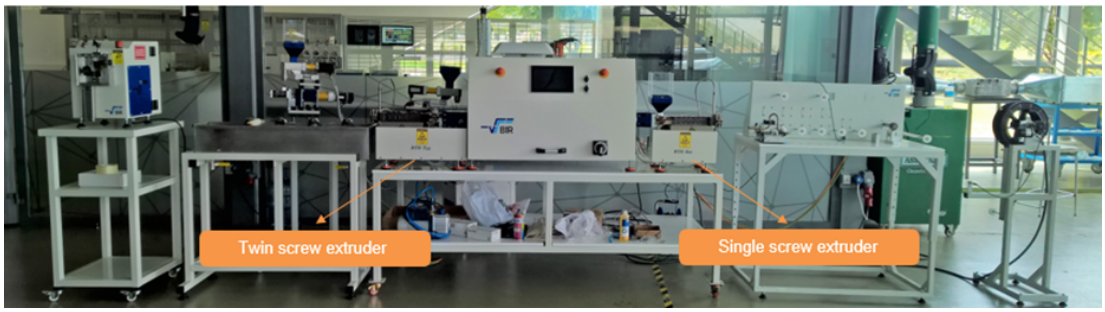

Figure 2.1 : Custom-made extruder.

Table 2.2 : Technical information for twin screw extruders.

Properties	Twin-Screw Extruder
Number of screws	2
Screw diameters	12 mm
Screw material	Nitrified carbon steel
L/D ratio	22
Rotation	Co-rotating
Motor power	1 kW
Speed range	1 to 350 rpm with 1 rpm precision
Max temperature	400 C
Pressure sensor	0-100 Bar with IP65 certification
Cooling	Air and water (main-feeder zone)
Side-feeder	2
Gravimetric feeders	2 (main and side feeders)

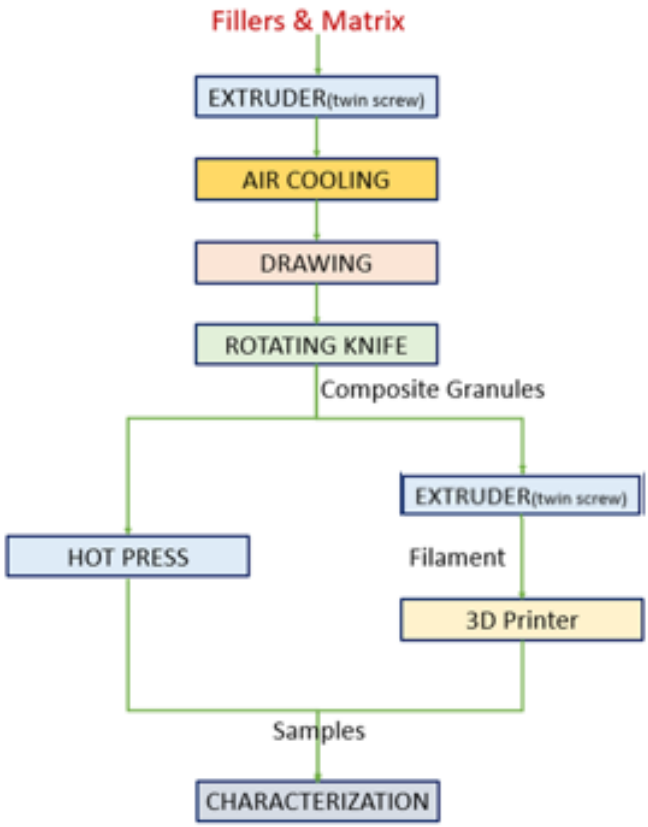

Figure 2.2 : Schematics illustrating the steps of fabrication process.

2.3.1 Fabrication of BN/PEI composites

Since PEI is highly susceptible to moisture absorption, all-polymer granules were dried in a convection oven at 150 °C overnight before the extrusion process. The custom-built co-rotating twin-screw extruder with a detailed schematics presenting all zones and feeding sections illustrated in Figure 2.3, was capable of fabricating composite granules, successfully. This work aimed to fabricate h-BN reinforced PEI composites with enhanced thermal conductivity as well as to investigate the role of processing conditions on the phonon transport mechanism.

Then, a parametric study was conducted to optimize the rotor speed, temperature and feeding rate conditions for achieving a proper dispersion state of BN as a filler in an amorphous high-performance polymer, PEI.

To minimize the interfacial phonon scattering mechanism, and tune the processing-dispersion and dispersion-thermal conductivity relation, BN/PEI polymer composites were fabricated with various rotor speeds from 50 rpm to 330 rpm, at different feeding rates as 0.5 kg/h to 1.5 kg/h and temperatures from 350 °C to 380 °C. Initially, we investigated the effect of rotor speed through keeping the feeding rate and the temperature constant/unvaried at 0.5 kg/h and temperature at 360 °C respectively. Then, the temperature effect was studied at a constant rotor speed of 250 rpm and feeding rate of 0.5 kg/h. Finally, the feeding rate effect was investigated at a 250 rpm rotor speed and temperature of 360 °C. Through these steps an optimum process condition was determined as 250 rpm rotor speed, 360 °C, and 1 kg/h feeding rate. Then, 5,10,15,20,25, and 30 wt.% BN/PEI composites were fabricated with optimum conditions.

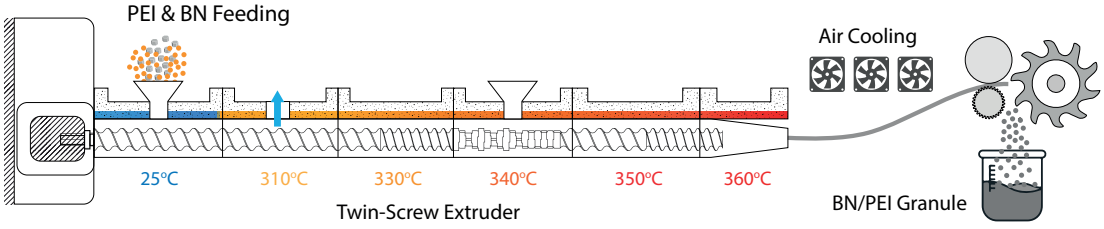

Figure 2.3 : Fabrication process for BN/PEI polymer composites.

2.3.2 Fabrication of CNTs/BN/PEI composites

Adding nano- and/or micro-scale fillers to high-performance polymers with minimal weight penalty can increase the intrinsic low thermal conductivity of thermoplastics. Reinforcing strategies through adding carbon (carbon nanotubes, graphene) or boron nitride (hexagonal-BN) based nano and micron-sized fillers which form percolated networks may help to perform well in high-end applications for thermal management. Several challenges associated with polymer composite filaments are expected to arise and result in lowering the overall thermal conductivities and mechanical properties. To overcome these challenges hybridization approaches such as using CNTs and BN simultaneously are offered. The hybrid polymer composite filaments using PEI matrices were given in Table 2.3 with their compositions and melt processing conditions. During melt processing/compounding, PEI and BN were added from the main feeder while CNTs were added from the side feeder as illustrated in Figure 2.4 in/under optimum conditions referred/determined as the rotor speed of 250 rpm and the temperature of 360 °C. The hybridized polymer filaments were referred to as CNTs/BN/PEI composites in this process.

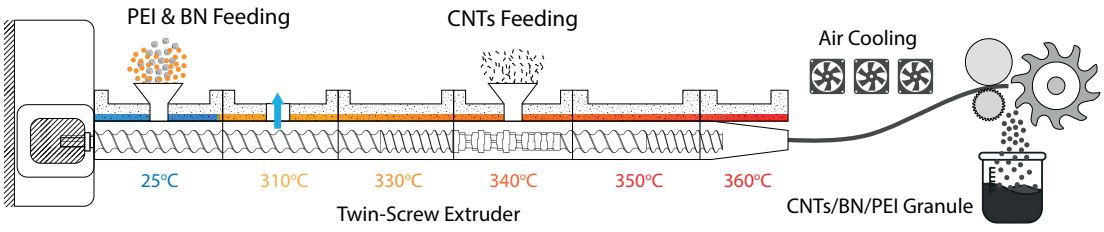

Figure 2.4 : Fabrication process for CNTs/BN/PEI polymer composites by melt compounding.

Table 2.3 : Samples of hybrid polymer composite filaments formed of CNTs/BN/PEI fabricated with optimized extrusion conditions.

Sample	CNTs content (wt. %)	BN content (wt. %)	PEI content (wt. %)	Temperature (°C)	Rotor Speed (rpm)	Main Feeder (kg/h)
1 wt. % CNTs/ 20 wt. % BN /PEI	1	20	79	360	250	1
2 wt.% CNTs/ 20 wt.% BN /PEI	2	20	78	360	250	1
1 wt.% CNTs/ 15 wt.% BN /PEI	1	15	84	360	250	1
2 wt.% CNTs/ 15 wt.% BN /PEI	2	15	83	360	250	1
5 wt.% CNTs/ 15 wt.% BN /PEI	5	15	80	360	250	1

2.3.3 Fabrication of BN/PEI and CNTs/BN/PEI composites for thermal conductivity measurements

The thermal conductivity measurement samples were fabricated by two different processes, that are (i) 3D-printing and (ii) hot-press. All composite compositions fabricated by twin-screw extrusion were granulated by a granulator. Then, obtained granules were used in filament fabrication and hot-press process. The single-screw extrusion (see Figure 2.5) was employed in filament fabrication with 60 rpm rotor speed at a drawing ratio of 20. Neat PEI, BN/PEI, and CNTs/BN/PEI filaments were successfully fabricated and presented in Figure 2.6. The fabricated filaments were used to fabricate as neat PEI, BN/PEI, and CNTs/BN/PEI samples by a custom-built high performance 3D printer in ITU ARC (Figure 2.7). 3D printed samples were shown in Figure 2.8. and hot pressed samples were presented in Figure 2.9. One particular reason to fabricate cylindirical discs for thermal conductivity measurements is to investigate the directional dependency of printed specimens when 3D printing is applied. The samples fabricated through compression molding was performed 300 °C and under a pressure of 2.5 MPa for 20 minutes for all neat PEI, BN/PEI, and

CNTs/BN/PEI samples. The resulting samples showed no voids or crack formation as depicted in Figure 2.10.

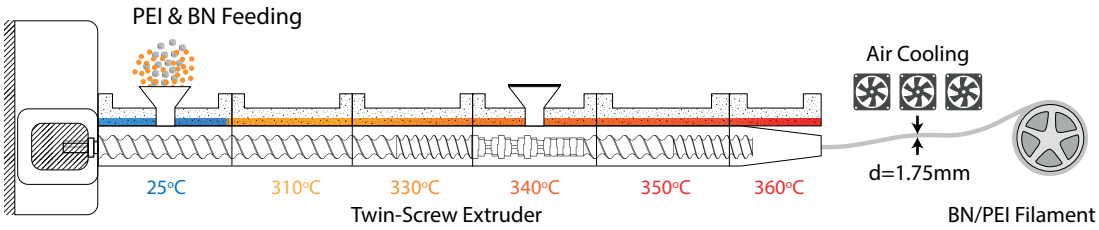

Figure 2.5 : Extrusion of composite filaments.

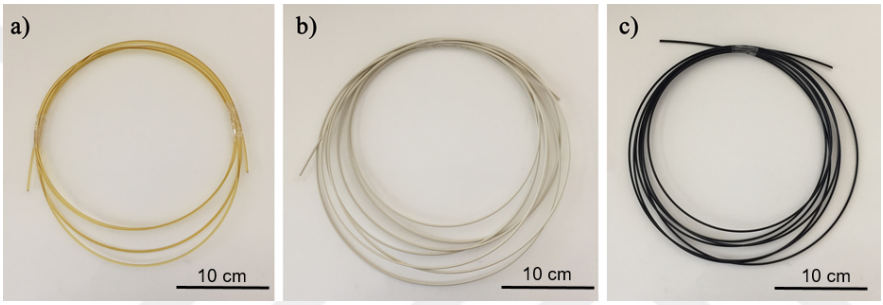

Figure 2.6 : a) neat PEI **b)** 20 wt.% BN/PEI and **c)** 1 wt.% CNTs/ 20wt.% BN/PEI filaments fabricated by extrusion.

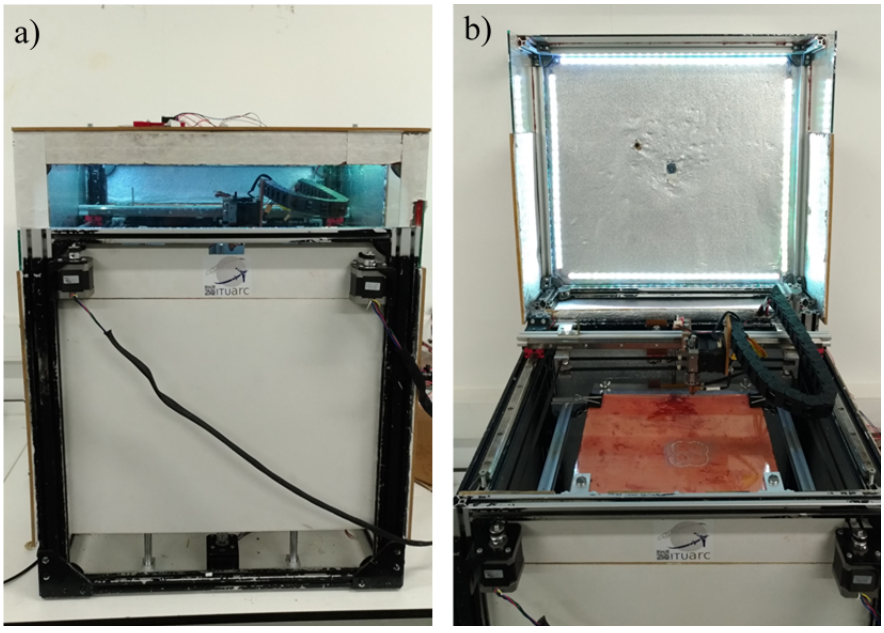

Figure 2.7 : ITUARC High-Performance 3D Printer **a)** Exterior view **b)** Interior view.

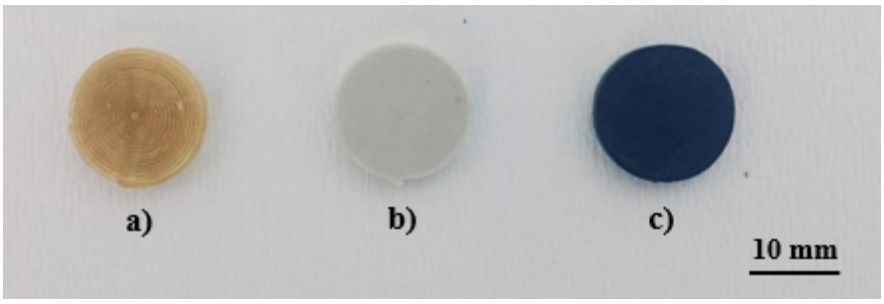

Figure 2.8 : 3D printed **a)** neat PEI, **b)** BN/PEI and **c)** CNTs/BN/PEI samples.

Figure 2.9 : Hot-press machine.

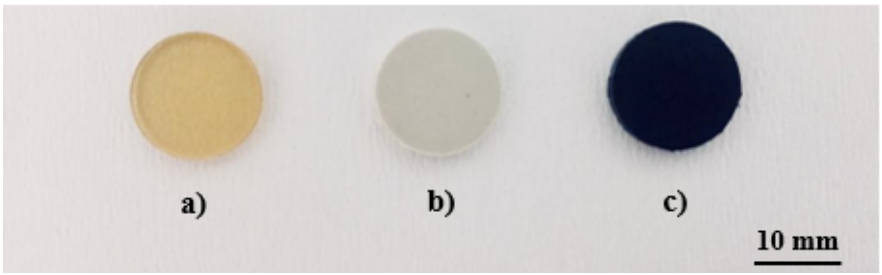

Figure 2.10 : Hot-pressed **a)** neat PEI, **b)** BN/PEI and **c)** CNTs/BN/PEI samples.

2.4 Characterization Methods

2.4.1 Thermal analysis

2.4.1.1 Differential scanning calorimetry

Differential scanning calorimetry (DSC) is a thermal analysis method which enables to determine the change of materials' heat capacity versus temperature. The heat capacity of the sample can be determined by change in mass during heating or cooling and variation in the heat flow. In this way, phase changes of a sample such as melting and glass transition temperature (*Tg*) are identified [70]. For the polymeric materials, *Tg* values determine the material's mechanical and physical properties. In this research, DSC measurements were performed on a TA Instrument DSC Q2000 thermal analyser at a heating rate of 10 °C/min. First, each sample was heated from 50 °C to 350 °C under an inert N_2 atmosphere to clear the thermal history of the samples. Then, they were cooled down fast to 50 °C and then they were reheated to 350 °C with a heating rate of 10 °C/min. The second heating scan was used for DSC analysis.

2.4.1.2 Thermogravimetric analysis

Thermogravimetric analysis (TGA) enables to determine the composition and thermal stability of a material. Through TGA, the rate of weight changes in a material as a function of temperature in air or inert atmospheres is defined. By establishing materials' decomposition and oxidation temperatures, the material selection processes for various applications can easily be handled [71]. TGA was using a TA Instrument-TGA55 at a heating rate of 10 °C/min under the nitrogen atmosphere within a temperature range of 30-800 °C. The measurements were conducted using samples with varying weights between 5 and 10 mg.

2.4.2 Morphological analysis

Scanning electron microscope (SEM) is a surface characterization method that allows the investigation of surface topography and composition of the sample. The column and the cabinet are the main parts of the SEM. The electrons traverse

throughout the column until they reach the sample. The detectors inside the column capture the scattered electrons from the sample. Then, the scattered electrons are transformed electrical signals to analyse images and graphs. Also, SEM consist of an electron source, electromagnetic lenses, electron detectors, sample chambers and computer [72]. The detailed working principle of SEM is shown in Figure 2.11. For morphological analysis, neat PEI, BN/PEI, and CNTs/BN/PEI composites were fractured under cryogenic atmosphere and their cross-sections were analysed by scanning electron microscopy (SEM) (Quanta FEG 450), operating at 15 keV. The fractured cross-section was then coated with gold-palladium alloy for 45 sec.

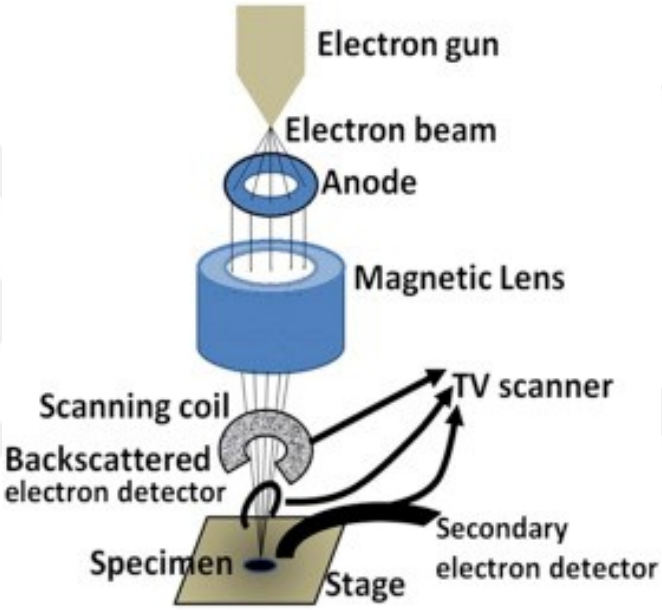

Figure 2.11 : Components of SEM [73].

2.4.3 Rheological Measurements

Rheology is frequently used to determine the flow behaviour of polymers when reinforcing through fillers is considered [74]. The main material parameters such as shear stress, shear rate, and viscosity are measured using torque and flow rate [75]. TA Discovery Hybrid Rheometer (Discovery HR) was used in this study, which allows to determine product viscosity and product properties such as storage modulus and loss modulus. Dynamic rheological measurements were performed by a TA Discovery HR-2 rheometer (Figure 2.12) using a parallel plate geometry (25 mm diameter and 1 mm gap). The samples were initially dried at 150 °C in a convection oven for overnight in order to prevent oxidation and were measured at 360 °C. First, strain sweep tests were performed to determine the linear viscoelastic region (LVR) and then frequency

sweep tests were carried out between 0.1 and 628 rad/s using a strain amplitude within the linear viscoelastic regime.

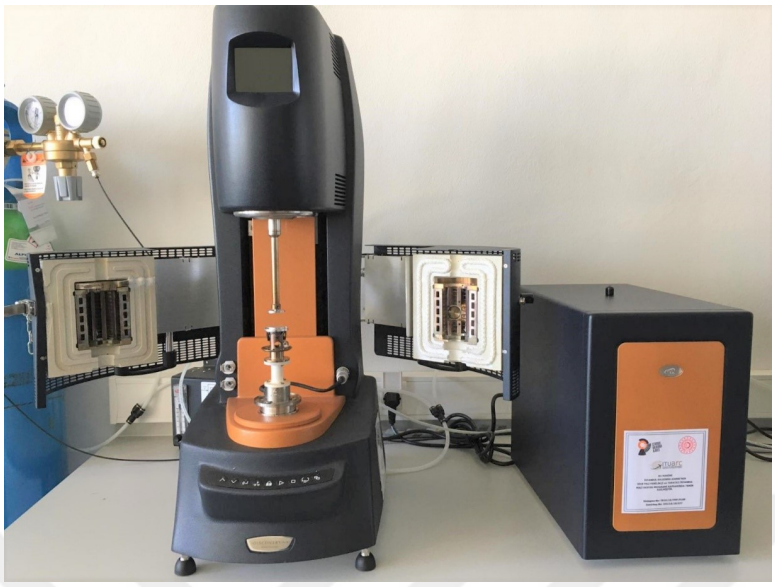

Figure 2.12 : TA Instrument HR-2.

2.4.4 Thermal conductivity measurements

Transient plane source (TPS) method which is commonly used to determine bulk materials thermal properties is considered for both neat PEI and BN/PEI and CNTs/BN/PEI composites. In this method, Kapton sensor is placed between two identical samples and power is applied. Then, the response of materials is recorded by measuring heat conductance. The thermal conductivity of composites was measured using a hot disc thermal analyser TPS 2500 S (Figure 2.13). The dimensions of the test specimens had a diameter of 15.6 mm and a thickness of 2 mm. The sensor supplied a heat pulse of 0.027 W for 10 s to the sample.

Figure 2.13 : Hot-disk TPS 2500S thermal conductivity measurement tool.

3. RESULTS AND DISCUSSION

3.1 Process Optimization for BN/PEI Composites

Melt compounding process was performed by utilizing a custom-built twin-screw extruder in here. The twin-screw extruder process can be controlled by three main parameters as rotor speed, feeding rate, and temperature. These three parameters can determine all flow characteristics of polymers [76]. Therefore, the parameters should be optimized for effective distribution and dispersion of the fillers. The microstructure and thermal behavior properties of composites were studied through rheological measurements to establish the processability of them when fillers were added to neat PEI matrix. Additionally, rheological investigations can yield valuable information about dispersion quality by investigating the storage modulus curve of the material. The generation of the plateau region at low frequencies indicates a formation of network structure when fillers were considered [77, 78]. In this scope, addition of BN to PEI matrix were studied at various weight and processing conditions. Effect of rotor speed, feeding rate and temperature were investigated to achieve a good dispersion and distribution of BN/PEI composites. All of the analysis were performed through rheological characterizations hence among the results 20 wt.% BN/PEI composites were identified as the best ratio for BN addition during the optimization experiments.

3.1.1 Effect of the rotor speed on the dispersion of BN in PEI matrix

The basic working principle of the twin-screw extruders is to apply high shear forces combined with heat to the polymer. Both polymer melting and dispersion of the fillers are affected by the screw rotor speed, feeding rate, and temperature; therefore, the determination of optimum parameters is very critical [80]. Hence, the polymer composites were fabricated with different rotor speeds from 50 rpm to 330 rpm with an increase of 40 rpm. The effect of the rotor speed on the storage modulus and complex viscosity were investigated and as presented in Figure 3.1(a) and Figure

3.1(b), respectively. The rotor speed has a drastic effect on the dispersion of BN in the PEI matrix as illustrated in Figure 3.1(a). The rotor speed optimization of the 20 wt.% BN/PEI composite was achieved under the conditions of 0.5 kg/h feeding rate and 360 °C die temperature. Figure 3.1(a) reveals that the low-frequency power-law dependence of G' decreases with increasing rotor speed up to 330 rpm hence the frequency dependence of the composites decreased. The terminal behaviour to nonterminal behaviour transition of the storage modulus can be attributed to increased dispersion quality. However, the effective BN dispersion was decreased when the rotor speed reached to 330 rpm and can be attributed to the reduction of mixing time. In addition, complex viscosity magnitudes, and shear thinning behaviour of the BN/PEI composite increased with increasing rotor speed up to 330 rpm as illustrated in Figure 3.1(b). Therefore, the most appropriate rotor speed was selected as 250 rpm. In addition, there was a minimal difference found between 250 rpm and 290 rpm while an important one was seen between 210 rpm and 250 rpm. When 250 rpm and 290 rpm are compared, it was clearly observed that at 290 rpm, the complex viscosity presented an critical enhancement than the storage modulus.

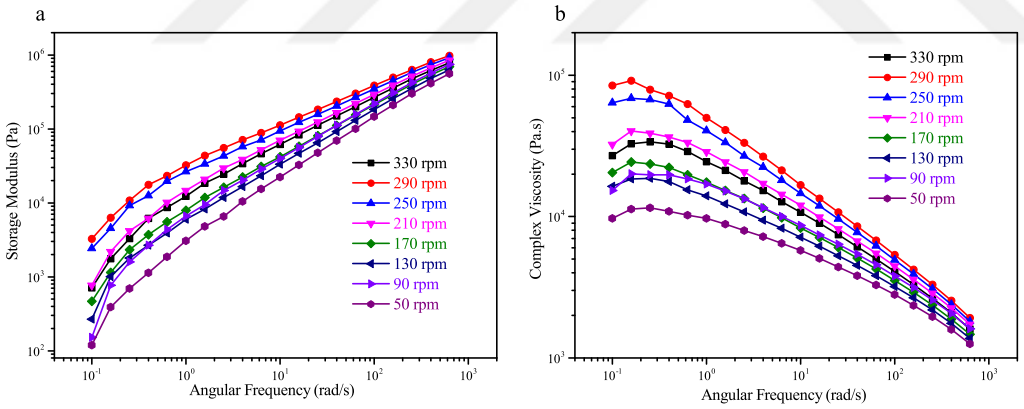

Figure 3.1 : (a) Storage modulus (G') and (b) complex viscosity (η^*) of 20 wt.% BN/PEI composites prepared with various rotor speeds with a die temperature of 360 °C .

3.1.2 Effect of the feeding rate on the dispersion of BN in PEI matrix

The feeding rate is another parameter in melt compounding that should be considered to achieve an effective dispersion. 20 wt.% BN/PEI composites were prepared with varying feeding rates to investigate their role in dispersion. The rheological measurements (Figure 3.2) showed that the feeding rate presented a great influence on the dispersion of BN fillers. When low frequencies were investigated, the best

dispersion quality was obtained under a feeding rate of 1 kg/h. The rheological differences that arose from various feeding rates can be associated with the residence time of the composites in the extrusion process. The optimum feeding rate was found to be 1 kg/h since the complex viscosity and storage modulus od 20 wt.% BN/PEI composites presented the best values as shown in Figure 3.2(a) and (b), respectively.

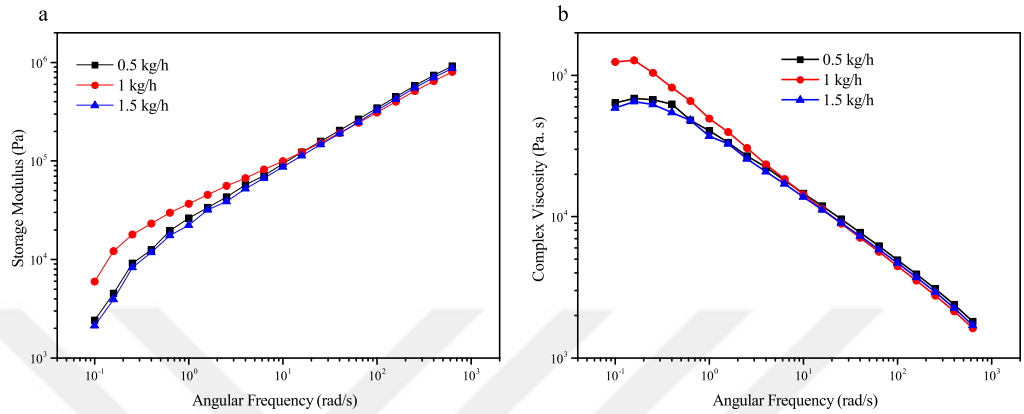

Figure 3.2 : (a) Storage modulus (G') and (b) complex viscosity (η^*) of 20 wt.% BN/PEI composites prepared with various feeding rates using twin-screw extruder operated at a screw speed of 250 rpm and a die temperature of 360 °C .

3.1.3 Effect of the temperature on the dispersion of BN in PEI matrix

The operating temperature has a significant effect on the dispersion quality of filler. The storage modulus (G') of the composites prepared at 360 °C was higher compared to the samples prepared at 370 °C and 380 °C as seen in Figure 3.3(a). This result showed that the stress applied during mixing has decreased when the temperature increased which caused a lowering effect on the viscosity. Therefore, the optimum temperature for BN/PEI composite fabrication was determined as 360 °C. After conducting the aforementioned optimization experiments, the optimum process conditions for BN/PEI polymer composites fabrication was found as 250 rpm screw speed, 1 kg/h feeding rate, and 360 °C of temperature. These optimum parameters were used to fabricate 5, 10, 15, 20, and 25 wt.% BN/PEI composites which were investigated with several characterization techniques and the results were presented in the following subsections.

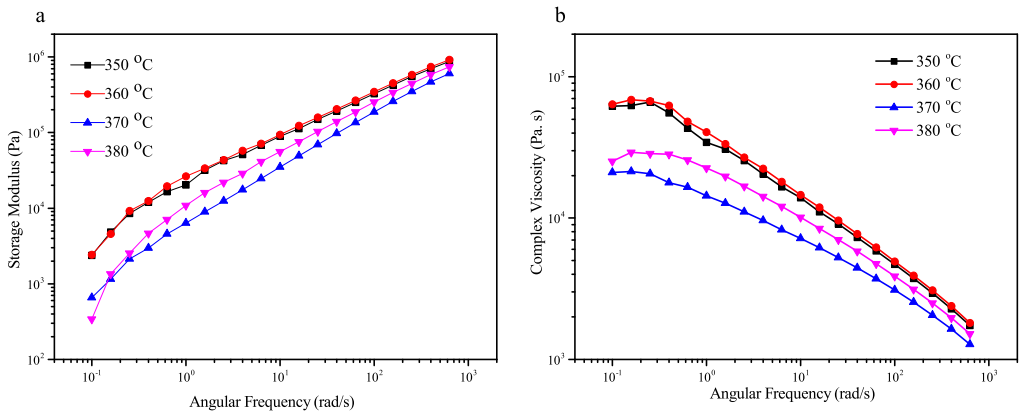

Figure 3.3 : (a) Storage modulus (G') and (b) complex viscosity (η^*) of 20 wt.% BN/PEI composites prepared at four different die temperatures, at a rotor speed of 250 rpm and 1 kg/h feeding rate.

3.2 Thermal Analysis of PEI and BN/PEI Composites

3.2.1 Thermal degradation analysis of PEI and BN/PEI composites

The thermal stabilities of the BN/PEI and CNTs/BN/PEI composites were characterized by TGA, and the results were presented in Figure 3.4 and Figure 3.5. The test conducted from 30 °C to 800 °C at a heating rate of 10 °C/min under the nitrogen atmosphere. The degradation temperatures corresponding to 5% and 15% weight losses were determined and named as T_5 and T_{15}. These degradation temperatures were used to characterize the thermal stabilities of the composites. The thermogravimetric analysis of the BN/PEI and CNTs/BN/PEI composites were also tabulated and reported in Table 3.1 and Table 3.2, respectively. Neat PEI showed a characteristic thermal decomposition of both aromatic and non-aromatic groups at around 500 °C and 550 °C, respectively. BN addition to neat PEI matrix did not result in a significant increase in the thermal stability. Nevertheless, an important increase in the decomposition temperatures was observed with BN filler addition. Degradation temperatures of T_5 and T_{15} of the neat PEI were found as 508 °C and 522 °C, respectively, which are the lowest ones found among all the fabricated composites. The addition of BN fillers led to 4 °C and 12 °C increases in the degradation temperatures of T_5 and T_{15} of BN/PEI composites, respectively. This behavior can be attributed to the high thermal stability of BN fillers as similar results were reported for BN dispersed polymer composites by several researchers [55, 79] . The residues and the residual amounts were associated with the presence of aromatic groups and the addition of

high-temperature resistance fillers to the PEI matrix, respectively. While the material residue was 46% for the neat PEI, the amount increased with increasing BN content and reached 70% for 25 wt.% BN/PEI composite. Therefore, the results prove that the thermal stability of PEI was increased with BN addition. Additionally, hybridization through CNTs addition was found to be ineffective on the thermal stability of the composites which can be attributed to low loadings of CNT content.

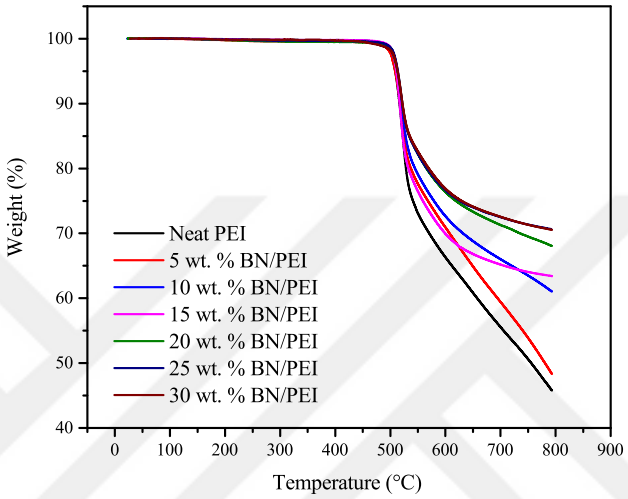

Figure 3.4 : TGA thermograms of neat PEI and BN/PEI composites.

Table 3.1 : TGA results of PEI and BN/PEI composites.

Material	T_{onset} (°C)	T_5 (°C)	T_{15} (°C)
Neat PEI	504.9	508.7	522.4
5 wt.% BN/PEI	503.2	508.7	524.5
10 wt.% BN/PEI	506.7	512.3	527.6
15 wt.% BN/PEI	506.0	510.6	522.3
20 wt.% BN/PEI	505.3	512.8	534.3
25 wt.% BN/PEI	506.2	513.5	534.3
30 wt.% BN/PEI	507.0	515.4	555.0

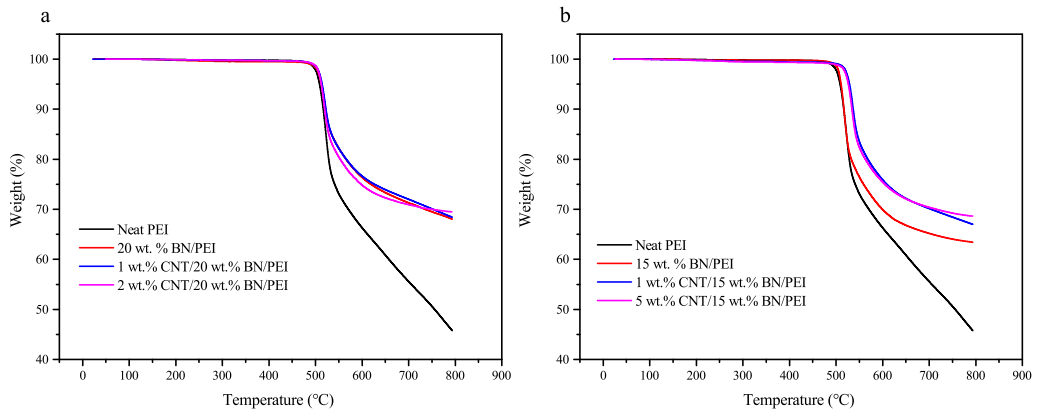

Figure 3.5 : Degredation effect of CNTs on a) 20 wt.% BN/PEI and b) 15 wt.% BN/PEI composites.

Table 3.2 : TGA results of neat PEI, BN/PEI and CNTs/BN/PEI composites.

Material	T_{onset} (°C)	T_5 (°C)	T_{15} (°C)
Neat PEI	504.9	20508.7	79522.4
20 wt.% BN/PEI	505.3	512.8	534.3
1 wt.% CNTs/20 wt.% BN/PEI	506.9	514.3	534.9
2 wt.% CNTs/20 wt.% BN/PEI	506.2	512.4	528.3
15 wt.% BN/PEI	505.9	510.6	522.3
1 wt.% CNTs/15 wt.% BN/PEI	522.9	528.6	545.0
5 wt.% CNTs/15 wt.% BN/PEI	521.0	526.2	541.1

3.2.2 Thermal transition analysis of BN/PEI and CNTs/BN/PEI composites

The thermal management materials should have high dimensional stability to work effectively and provide confidence [80]. Therefore, the glass transition temperatures (*Tg*) of the composites were investigated by DSC with a heating rate of 10 °C/min between 50 °C and 350 °C. The second heating scan of DSC thermograms of the BN/PEI and CNTs/BN/PEI composites were shown in Figure 3.6 and 3.7, respectively. *Tg* of the neat PEI, BN/PEI and CNTs/BN/PEI composites were found as 217 °C and 215 °C, respectively. This behaviour pointed out that BN and CNTs addition did not affect the local motion of the polymer chains which can be associated with the entanglement length of the polymer chains. Therefore, it can be interpreted as BN and CNTs addition cannot hinder the motion of polymer chains. Similar behavior was also reported by Ghose et. al. [81] in which high loadings of 20 wt. % CNTs and 30 wt. % carbon nanofibers (CNFs) were used as fillers in the PEI matrix by melt compounding and no significant kinetic thermal transitions were found. Both of the findings through

TGA and DSC analyzes could be interpreted as that BN and CNTs addition had a minimal effect on the processability during hot-press processes.

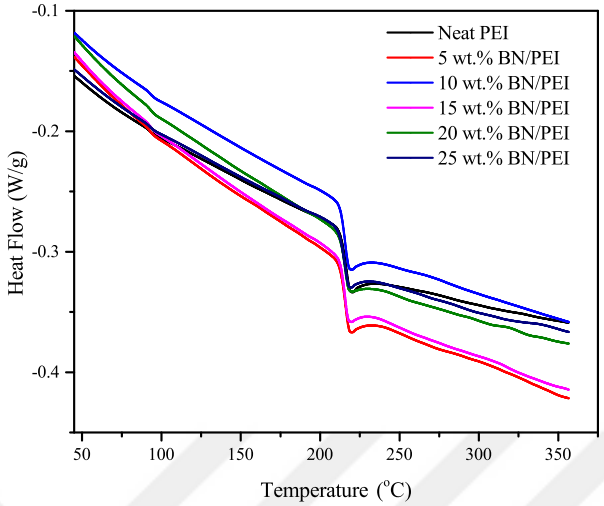

Figure 3.6 : DSC analysis of neat PEI and BN/PEI polymer composites.

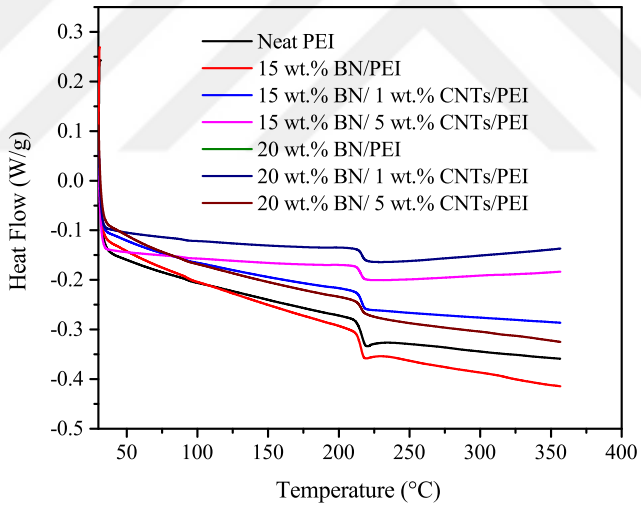

Figure 3.7 : DSC analysis of neat PEI and CNTs/BN/PEI composites.

3.3 Rheological Measurements

3.3.1 Rheological effect of BN addition

The dynamic frequency sweep test is a suitable way to investigate the microstructure and network between matrix and fillers of the composites. The rheological curves of the neat PEI and BN/PEI composites are shown in Figure 3.8. The frequency-dependent storage moduli (G') of the neat PEI and BN/PEI composites were shown in Figure 3.8(a). The neat PEI and BN/PEI composites with low BN loadings

found to be obeying the scaling law ($G' \sim \omega^2$ and $G'' \sim \omega^1$). On the other hand, when the BN concentration was higher than 15 wt.%, this terminal behaviour disappeared, and this situation can be explained with a shift from liquid- to solid-like viscoelastic behavior. Moreover, with higher BN addition than 15 wt.%, the polymer relaxations were prevented by the filler-filler interactions among BN micro-powders. This critical composition at 15 wt.% can be determined as the rheological percolation threshold concentration and also, after the rheological percolation threshold, the filler-filler network was compromised. The complex shear viscosity curve of the neat PEI and BN/PEI composites are shown in Figure 3.8(b). The complex shear viscosity was increased with increasing BN loading, presenting a Newtonian-like behavior at relatively low BN concentrations up to 15 wt.%. However, at higher concentrations, the behavior of the composites changed substantially and strongly shear-thinning was observed. The composite containing 20 wt.% BN, was two orders of magnitude more viscous than the neat PEI. The significant differences with higher BN concentrations than 15 wt.% were attributed to the changes in the microstructural composition and material properties. In addition, the increase in the complex viscosity did not create a drawback for hot-press processes as non-uniform distribution and agglomerate formation were not observed.

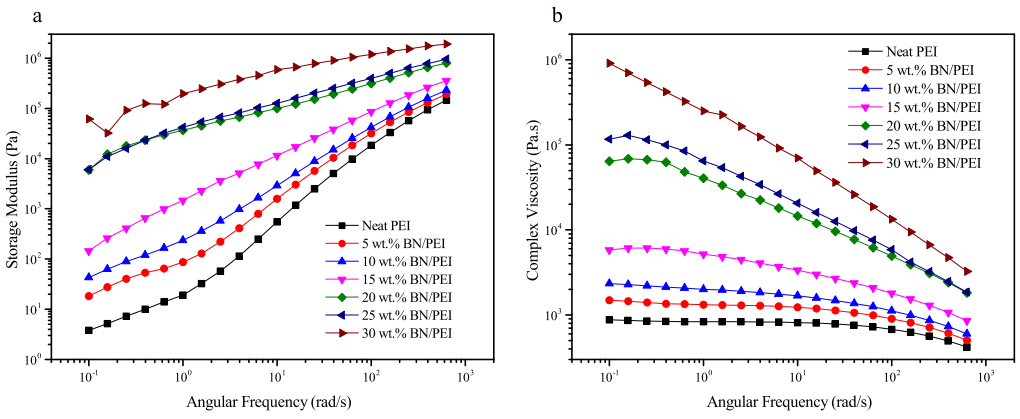

Figure 3.8 : (a) storage modulus and (b) complex viscosity of the neat PEI and BN/PEI composites as a function of frequency at 360 °C.

3.3.2 Rheological effect of CNTs addition

Rheological measurements were performed to analyze the effect of CNTs and addition to BN/PEI polymer composites and it was clearly seen in Figure 3.9. CNTs addition had an enormous effect both on the storage modulus and complex viscosity of CNTs/BN/PEI polymer composites as shown in Figure 3.9. The resulted in three orders

of magnitude increase may be associated with the influence of high aspect ratio CNTs presence by limiting the polymer chain mobility at low frequencies as shown in Figure 3.9(a). Additionally, composites showed strongly shear-thinning behavior as presented in Figure 3.9(b). However, the rheological measurements of 2 wt. %CNTs/20 wt. %BN/PEI and 5 wt. %CNTs/15 wt. %BN/PEI composites could not be performed due to high-temperature resistance of polymer composites.

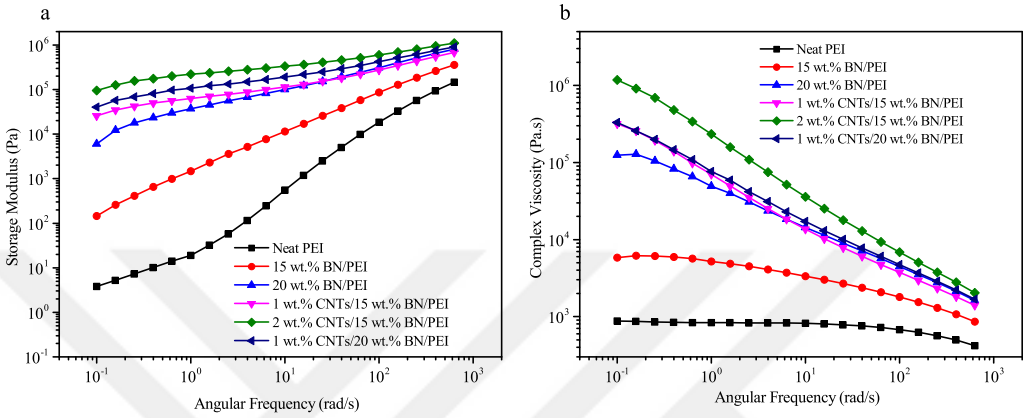

Figure 3.9 : (a) Storage modulus and (b) complex viscosity of BN/PEI and CNTs/BN/PEI composites, as a function of frequency at 360 °C.

3.4 Morhological Analysis

The microstructure of the BN/PEI and CNTs/BN/PEI composites was investigated using SEM in order to investigate the influence of filler morphology on thermal conductivity properties. Figure 3.10 illustrates the SEM micrograph of 20 wt.% BN/PEI composites in which one of them was fabricated at optimum processing conditions while the other one was prepared at non optimal conditions: 50 rpm rotor speed, 0.5 kg/h feeding rate and 360 °C. It was seen from Figure 3.10(a) that the BN particles disperse more homogeneously in PEI matrix and BN particles could touch each other and thermal conductive pathways formed due to applying high shear forces during extrusion. On the other hand, Figure 3.10(b) demonstrated that BN fillers could not find the necessary energy to homogeneously dispersion in high viscous PEI matrix and conductive pathways could not be formed.

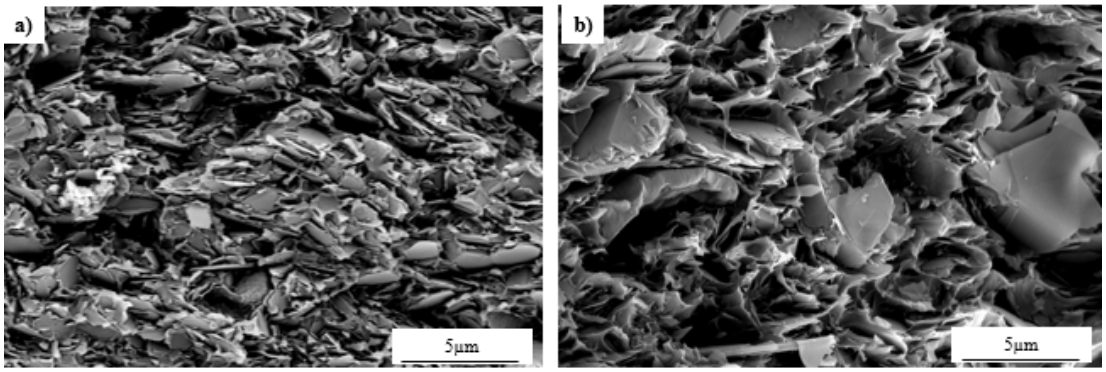

Figure 3.10 : SEM images of a) 20 wt.% BN/PEI (optimum conditions) and b) 20 wt.% BN/PEI (non optimal conditions).

The SEM images of neat PEI and BN/PEI composites with 15, 20 and 30 wt.% fractions were shown in Figure 3.11. At a moderately high filler loading of 30 wt.% BN/PEI polymer composites demonstrated that with the increasing BN concentration, BN particles were packed densely such as decreasing the particle-particle distance which leads to the formation of thermally conductive pathways for effective phonon transport (Figure 3.11(b)). However, when lower BN loadings were investigated, non-uniformly packed particles in PEI matrix were observed. Hence, the increased thermal conductivity can be attributed to decreasing distance between filler and matrix in polymer composites.

The SEM images of the PEI composites with the 20 wt.% BN and 1 wt.% CNTs/20 wt.% BN hybrid fillers were shown in Figure 3.12. When the CNTs/BN/PEI hybrid composites were investigated, it was observed that CNTs in the 20 wt.%BN/PEI composites could not construct bridge between BN fillers and heterogeneously dispersed. The SEM images showed that expected flat morphology could not be obtained.

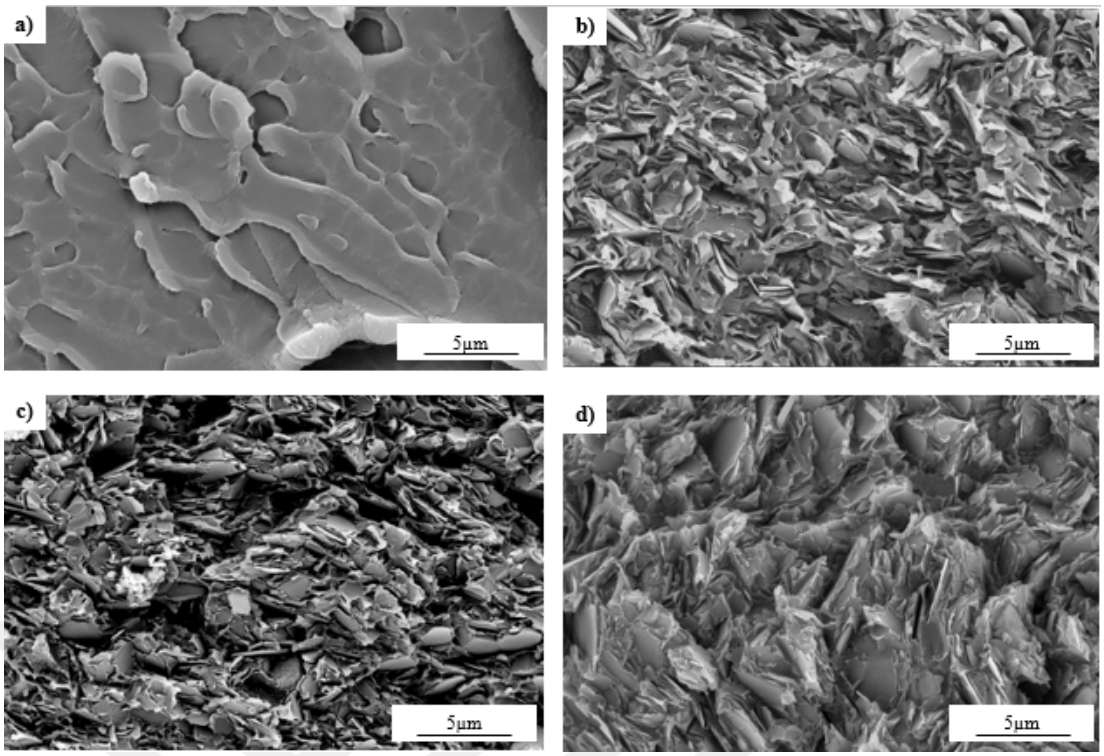

Figure 3.11 : SEM images of a) neat PEI b) 15 wt.% BN/PEI c) 20 wt.% BN/PEI d) 30 wt.% BN/PEI composites.

Lastly, morphology investigation applied to PEI composites which contained CNTs and 15 wt.% BN as illustrated in Figure 3.13. Also, SEM images of 15 wt.% and 20 wt.% BN/CNTs composites at higher magnification demonstrated in Figure 3.14, suggesting that CNTs addition construct bridges between BN fillers. Figure 3.14(a) and (c) reveals the CNTs addition led to be formed different morphology for 20 wt.%BN/PEI and 15 wt.% BN/PEI composites. The flat interface morphology of consist 1 and 5 wt.% CNTs/BN/PEI as demonstrated in Figure 3.13(c) and Figure 3.13(d), respectively. Besides, any agglomeration did not observed as in literature [82, 83]. Therefore, comprise of the thermal conductive pathway was achieved on the contrary that of 1 wt.% CNTs/20 wt.% BN/PEI composites.

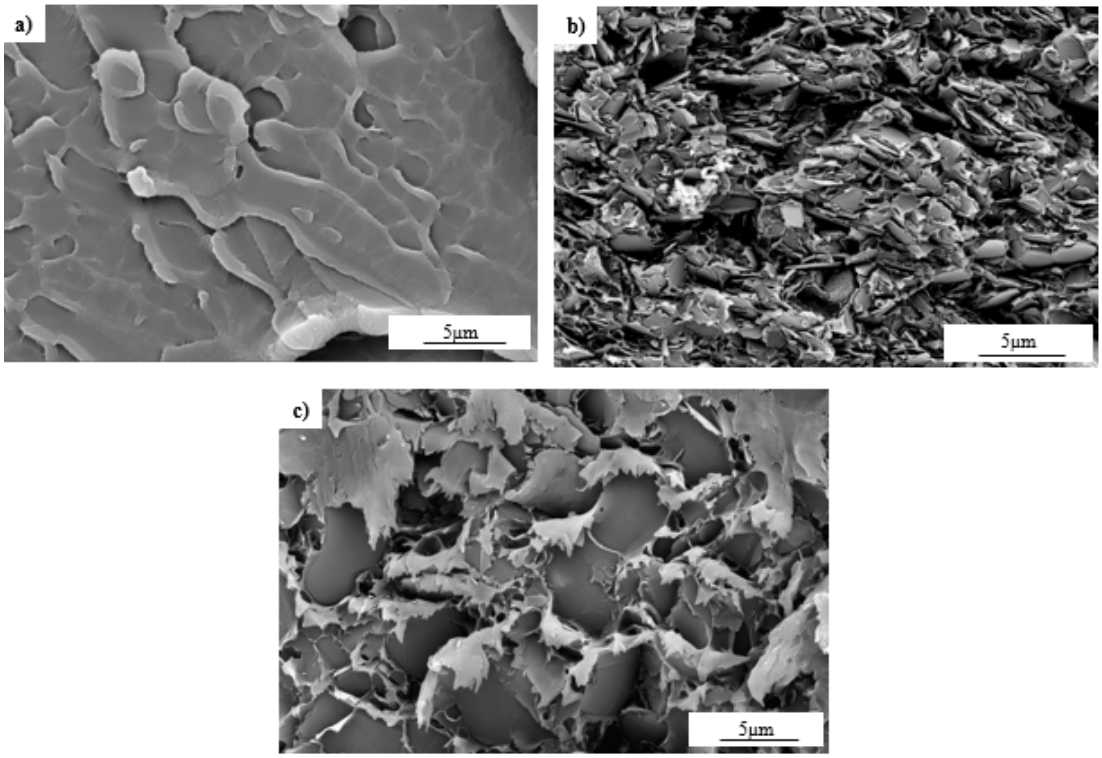

Figure 3.12 : SEM images of a) neat PEI, b) 20 wt.% BN/PEI and c) 1 wt.% CNTs/20 wt.%BN/PEI composites.

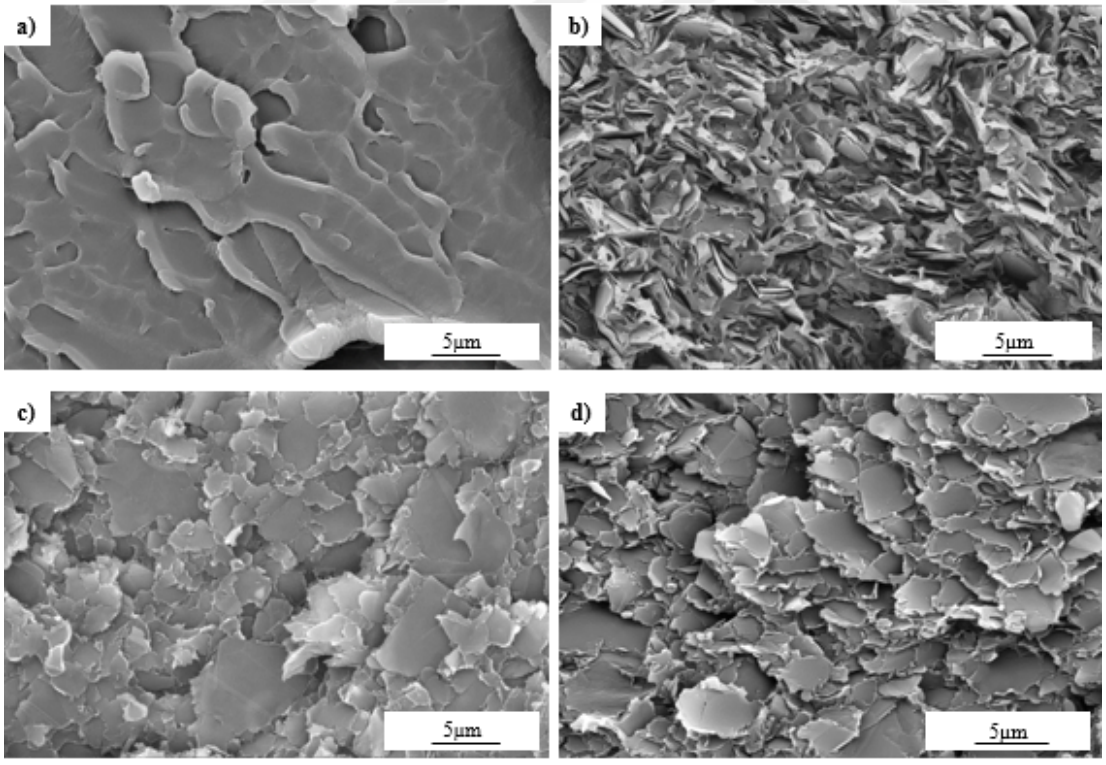

Figure 3.13 : SEM images of a) neat PEI, b) 15 wt.% BN/PEI and c) 1 wt.% CNTs/15 wt.%BN/PEI and d) 5 wt.% CNTs/15 wt.% BN/PEI composites.

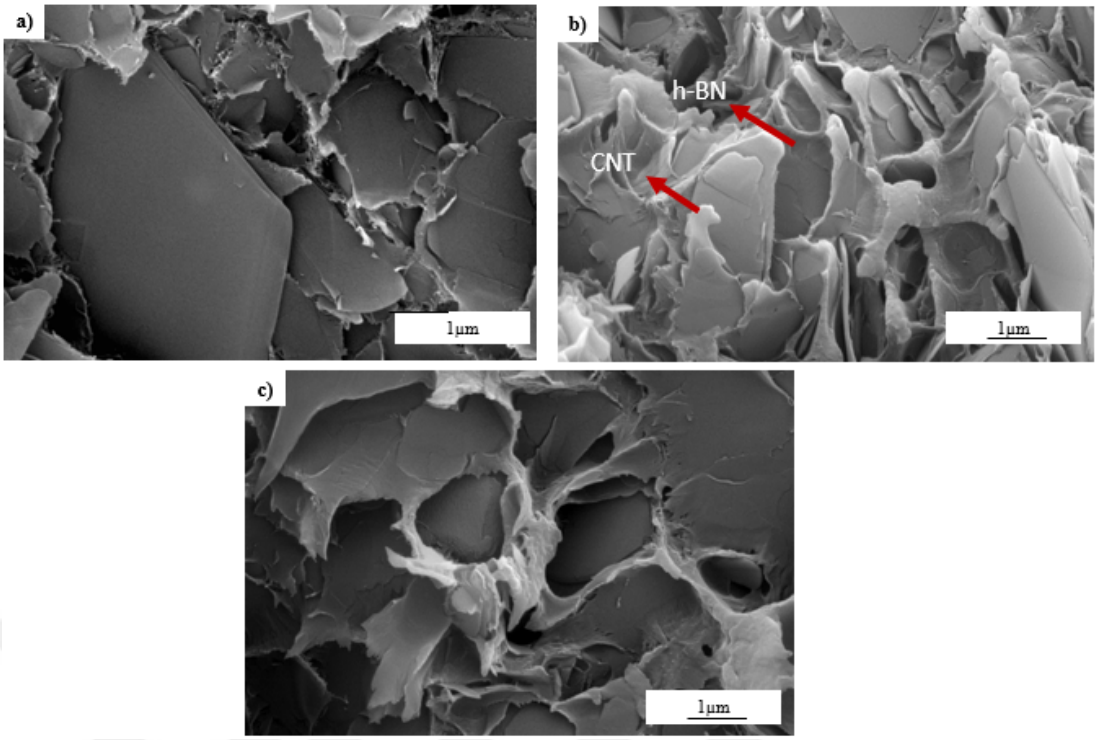

Figure 3.14 : SEM images of a) 1 wt.% CNTs/15 wt.%BN/PEI, b) 5 wt.% CNTs/15 wt.% BN/PEI and c) 1 wt.% CNTs/20 wt.%BN/PEI composites.

3.5 Thermal Conductivity Measurements

3.5.1 Influence of the dispersion on thermal conductivity

The correlation between storage modulus and thermal conductivity was investigated and shown together in Figure 3.15. The figure presents the storage modulus of BN/PEI composites at 0.1 rad/s and reveals the effect of the processing conditions on the thermal conductivity. The changing processing conditions such as rotor speed, feeding rate, and temperature led to a change in the dispersion quality as explained in the previous section. Therefore, it can be seen that the thermal conductivity pattern followed the same pattern as the storage modulus graph. The thermal conductivity results showed that changing dispersion quality affected the thermal conductivity. Figure 3.15(a) shows that thermal conductivity increased with increasing rotor speed up to 330 rpm. The increasing rotor speed created augmented shear force on polymers thus BN fillers can be dispersed more effectively. However, when the rotor speed reached 330 rpm the thermal conductivity and storage modulus of the sample decreased due to the generated high shear forces. Therefore, 6% increase in the thermal conductivity was achieved by changing the rotor speed from 50 rpm to 250 rpm.

Also, the feeding rate had an effect on the thermal conductivity results as seen in Figure 3.15(b). Three different feeding rates were studied in order to determine the optimum process conditions for the highest achievable thermal conductivity value. The feeding rates directly affected the residence time of the polymer and fillers. Indirectly increasing the residence time by shifting the feeding rate from 0.5 to 1 kg/h yielded an increase in the thermal conductivity and storage modulus values. Nevertheless, increasing the residence time caused a decrease in thermal conductivity and storage modulus values. Both the highest thermal conductivity value and storage modulus magnitude were achieved with 1 kg/h feeding rate. The third parameter in extruder systems affecting the thermal conductivity of the produced composites is the temperature. Figure 3.15(c) shows the thermal conductivity and storage modulus magnitudes (tested at 0.1 rad/s angular frequency) of the samples produced with three different temperatures. Increasing the temperature from 350 °C to 360 °C showed a minimal positive effect on the thermal conductivity and dispersion quality. However, increasing the temperature from 360 °C to 380 °C decreased the thermal conductivity and dispersion quality. This negative influence can be associated with the reduced shear forces due to increased temperatures. Thus, the highest thermal conductivity value, 0.6848 W/m K was achieved at 360 °C.

The thermal conductivity results and rheological measurements showed that the formation of thermal conductivity pathways and increasing dispersion quality followed similar patterns. The increasing dispersion quality of the BN/PEI composites resulted in an increase in the thermal conductivity by generating thermal conductivity pathways. Therefore, thermal conductivity results were shown to be open for improvement by tuning the processing conditions. Interestingly and more importantly, when the rheological measurements and the thermal conductivity results were compared, a correlation between the thermal conductivity and storage modulus was present. This correlation stated that when the dispersion quality was increased, the thermal conductivity and the storage modulus followed a similar trend.

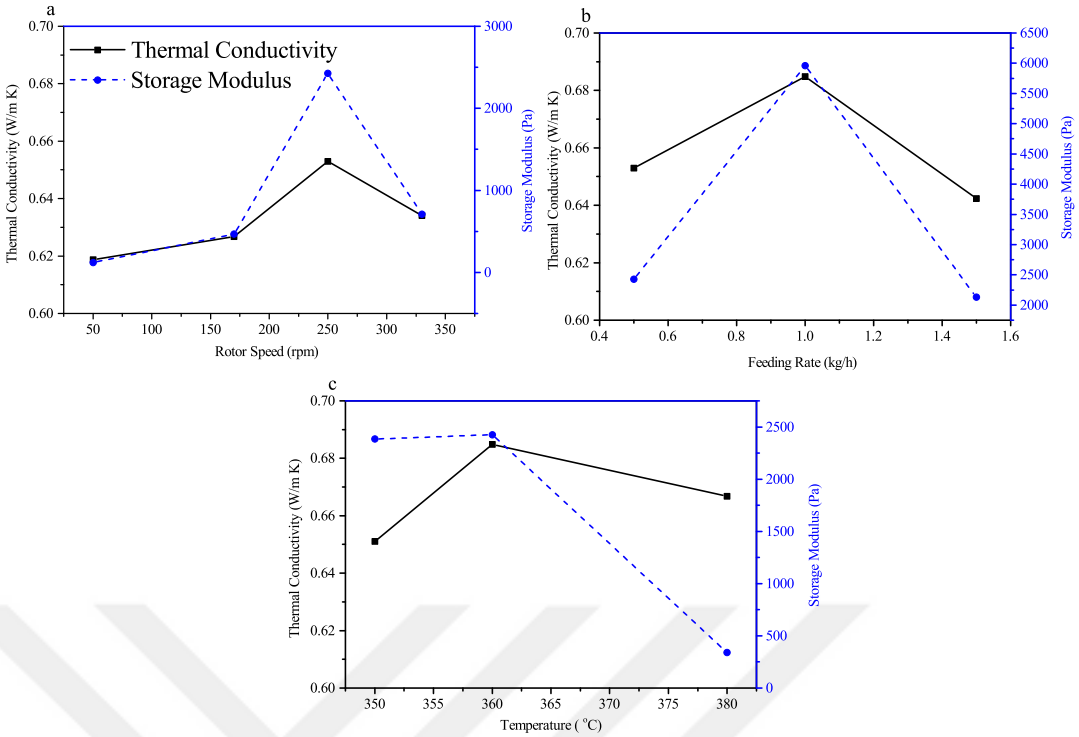

Figure 3.15 : Thermal conductivity values and storage modulus magnitudes (tested at 0.1 rad/s angular frequency) of 20 wt.% BN/PEI composites at various processing conditions.

3.5.2 Effect of the BN content on the thermal conductivity

The thermal conductivity of BN was much higher than PEI; therefore, the addition of BN fillers into the PEI matrix boosted the thermal conductivity of BN/PEI composites. Figure 3.16 shows the thermal conductivities of BN/PEI composites as a function of the BN content. The thermal conductivity of the neat PEI was obtained as 0.21 W/m K, which is the same value as given in the product technical data sheet. The thermal conductivities of BN/PEI composites were increased by 147% increase with the addition of 15 wt.% BN compared to neat PEI. When the BN concentration reached 30 wt.% the thermal conductivities of the composites increased by 285% which can be associated with the formation of an effective thermal conductivity network through establishing filler-filler interaction.

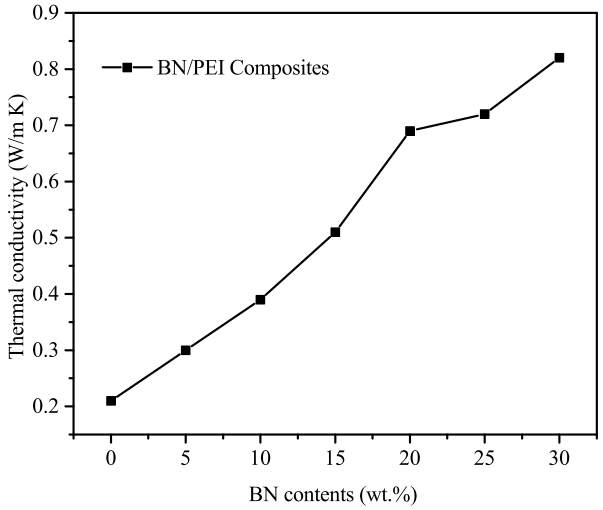

Figure 3.16 : Thermal conductivity of BN/PEI composites as a function of BN content.

3.5.3 Effect of the CNTs content on the thermal conductivity

Three-dimensional thermal transfer pathways may show a synergistic improvement on the thermal conductivity of polymer composites. Therefore, the addition of CNTs to BN/PEI polymer composites was considered to achieve a hybrid approach to enhance the thermal conductivity of these polymer composite filaments. CNTs with extremely high aspect ratio and intrinsic thermal conductivities were added to BN/PEI composites from 1 to 5 wt.%. while the BN content was 15 and 20 wt.%. When the intrinsic thermal conductivities of CNTs and BN considered, insufficient improvement was achieved and tabulated and illustrated in Table 3.3 and Figure 3.17, respectively. For 20 wt.% of BN/PEI was reinforced with CNTs from 0.5 to 2 wt.%, the decrease in the thermal conductivities of polymer composites may be attributed to the low contact area and weak interaction between BN to CNTs and/or CNTs to CNTs. Another possible reason may also be associated with the overloading of the composite system where CNTs acted like defects in polymer due to the high loading of fillers. Thermal conductivities of 15 wt.% BN/PEI were measured as 0.51 W/m K and increased to 0.81 W/m K when 5 wt.% CNT was added at the highest content. This increase clearly demonstrated the effect of hybridization through synergistic effects however the polymer composites were lack of printability. Novel studies to overcome this challenge will be performed by changing the nano- and micron-sized particles to fabricate polymer composite filaments.

Table 3.3 : Thermal conductivities of BN/PEI and CNTs/BN/PEI composites.

Hybrid Filler Contents		Thermal Conductivity
CNTs wt.%	BN wt.%	(W/m K)
-	20	0.68
1	20	0.65
2	20	0.62
-	15	0.51
1	15	0.54
2	15	0.59
5	15	0.81

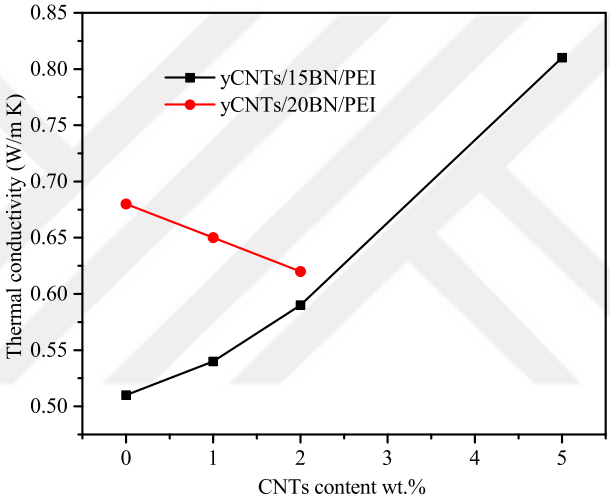

Figure 3.17 : Thermal conductivities of CNTs/BN/PEI composites as a function of CNT content.

3.6 Heat Sink Fabrication

The fabricated polymer composites showed that PEI matrix composites have suitable flow properties and offers an opportunity for the fabrication of thermally conductive, injection moldable, and 3D printable PMCs. In this context, fabricated 5 wt.% BN/PEI composite filaments (Figure 3.18) were used as feedstock materials for 3D-printing process and a heat sink model fabrication was achieved. The fabricated heat sink has 1 mm fin thickness and 3 mm distance between each fin as demonstrated in Figure 3.19. The 3D-printing process was achieved under 380 °C nozzle temperature, 150 °C bed temperature and 90 °C chamber temperature with a printing speed of 40 mm/s.

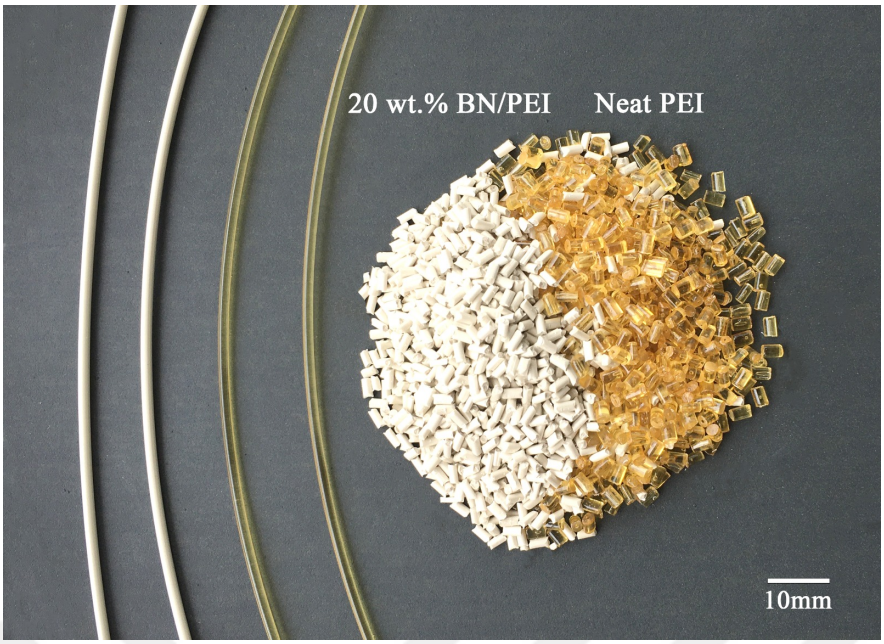

Figure 3.18 : BN/PEI composite granules and filaments.

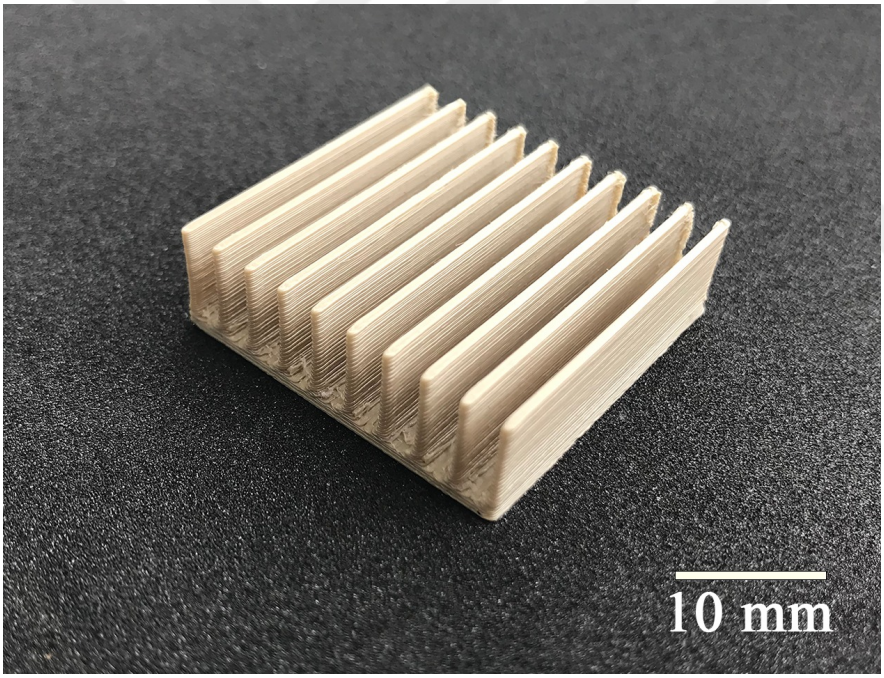

Figure 3.19 : 3D-printed heat sink model using BN/PEI filament.

4. CONCLUSION

In this thesis, neat PEI, BN/PEI, and CNTs/BN/PEI composite filaments at different fractions were successfully fabricated by melt compounding technique. Firstly, it was aimed to fabricate tailor melt processing of PEI with BN reinforcement to fabricate BN/PEI composites with enhanced thermal conductivity and understand the role of processing conditions on the dispersion and phonon transport mechanisms. The process carried out involved a parametric study to optimize the rotor speed, temperature, and feeding rate conditions for achieving a proper dispersion state of BN as a filler in an amorphous high performance polymer, PEI. To minimize the interfacial phonon scattering mechanism, and engineer the processing-dispersion and dispersion-thermal conductivity relation, BN/PEI polymer composites were fabricated with different rotor speeds (from 50 rpm to 330), different feeding rates (from 0.5 kg/h to 1.5 kg/h) and different temperatures (from 350 °C to 380 °C). The results exposed that optimization of melt compounding parameters; rotor speed, feeding rate, and temperature led to a %6 increase in thermal conductivity for each parameter.

The rheological measurements of BN/PEI composites were investigated with dynamic frequency sweep tests and the results showed that 15 wt.% BN concentration can be considered as the rheological percolation threshold. After this threshold point, polymer microstructure showed solid-like viscoelastic behaviour. It is noteworthy to mention that this microstructure change was detected in the thermal conductivity measurements. 15 wt.% BN/PEI composites showed 147% increase, although 25 wt.% BN/PEI composites showed 248% increase compared to neat PEI, resulting in thermal conductivity of 0.7167 W/m K. Furthermore, thermal conductivity measurements revealed that incorporation of 30 wt.% BN with optimum parameters led to 289% increase in thermal conductivity. Rheological measurements revealed that the flow

behaviour of CNTs/BN/PEI was changed remarkably with the addition of 1 wt.%CNTs and these amounts were determined as percolation thresholds.

REFERENCES

[1] **Moore, A.L. and Shi, L.** (2014). Emerging challenges and materials for thermal management of electronics, *Materials today*, *17*(4), 163–174.

[2] **Vadivelu, M.**, **Kumar, C.R. and Joshi, G.M.** (2016). Polymer composites for thermal management: a review, *Composite Interfaces*, *23*(9), 847–872.

[3] **Kim, H.S.**, **Jang, J.u.**, **Lee, H.**, **Kim, S.Y.**, **Kim, S.H.**, **Kim, J.**, **Jung, Y.C. and Yang, B.J.** (2018). Thermal management in polymer composites: a review of physical and structural parameters, *Advanced Engineering Materials*, *20*(10), 1800204.

[4] **Hussain, A.R.J.**, **Alahyari, A.A.**, **Eastman, S.A.**, **Thibaud-Erkey, C.**, **Johnston, S. and Sobkowicz, M.J.** (2017). Review of polymers for heat exchanger applications: Factors concerning thermal conductivity, *Applied thermal engineering*, *113*, 1118–1127.

[5] **Wong, K.V. and Hernandez, A.** (2012). A review of additive manufacturing, *International scholarly research notices*, *2012*.

[6] **Due, J. and Robinson, A.J.** (2013). Reliability of thermal interface materials: A review, *Applied Thermal Engineering*, *50*(1), 455–463.

[7] **Sarvar, F.**, **Whalley, D.C. and Conway, P.P.** (2006). Thermal interface materials-A review of the state of the art, *2006 1st Electronic Systemintegration Technology Conference*, volume 2, IEEE, pp.1292–1302.

[8] **Chen, X.**, **Su, Y.**, **Reay, D. and Riffat, S.** (2016). Recent research developments in polymer heat exchangers–A review, *Renewable and Sustainable Energy Reviews*, *60*, 1367–1386.

[9] **Githens, R.** (1965). Flexible-tube heat exchangers, *Chem. Eng. Prog.*, *61*, 55–62.

[10] **Pordanjani, A.H.**, **Aghakhani, S.**, **Afrand, M.**, **Mahmoudi, B.**, **Mahian, O. and Wongwises, S.** (2019). An updated review on application of nanofluids in heat exchangers for saving energy, *Energy Conversion and Management*, *198*, 111886.

[11] **Rengier, F.**, **Mehndiratta, A.**, **Von Tengg-Kobligk, H.**, **Zechmann, C.M.**, **Unterhinninghofen, R.**, **Kauczor, H.U. and Giesel, F.L.** (2010). 3D printing based on imaging data: review of medical applications, *International journal of computer assisted radiology and surgery*, *5*(4), 335–341.

[12] **Wang, X.**, **Jiang, M.**, **Zhou, Z.**, **Gou, J. and Hui, D.** (2017). 3D printing of polymer matrix composites: A review and prospective, *Composites Part B: Engineering*, *110*, 442–458.

[13] **Sood, A.K.**, **Ohdar, R.K. and Mahapatra, S.S.** (2010). Parametric appraisal of mechanical property of fused deposition modelling processed parts, *Materials & Design*, *31*(1), 287–295.

[14] **Hwang, S.**, **Reyes, E.I.**, **Moon, K.s.**, **Rumpf, R.C. and Kim, N.S.** (2015). Thermo-mechanical characterization of metal/polymer composite filaments and printing parameter study for fused deposition modeling in the 3D printing process, *Journal of Electronic Materials*, *44*(3), 771–777.

[15] **Liu, J.**, **Li, W.**, **Guo, Y.**, **Zhang, H. and Zhang, Z.** (2019). Improved thermal conductivity of thermoplastic polyurethane via aligned boron nitride platelets assisted by 3D printing, *Composites Part A: Applied Science and Manufacturing*, *120*, 140–146.

[16] **Lebedev, S.**, **Gefle, O.**, **Amitov, E.**, **Berchuk, D.Y. and Zhuravlev, D.** (2017). Poly (lactic acid)-based polymer composites with high electric and thermal conductivity and their characterization, *Polymer Testing*, *58*, 241–248.

[17] **Han, Z. and Fina, A.** (2011). Thermal conductivity of carbon nanotubes and their polymer nanocomposites: A review, *Progress in polymer science*, *36*(7), 914–944.

[18] **Ashcroft, N.W. and Mermin, N.D.** (1976). Solid State Physics (Holt Rinehart Winston, New York), *Google Scholar*.

[19] **Mehra, N.**, **Mu, L.**, **Ji, T.**, **Yang, X.**, **Kong, J.**, **Gu, J. and Zhu, J.** (2018). Thermal transport in polymeric materials and across composite interfaces, *Applied Materials Today*, *12*, 92–130.

[20] **Kim, W.** (2015). Strategies for engineering phonon transport in thermoelectrics, *Journal of Materials Chemistry C*, *3*(40), 10336–10348.

[21] **Xu, Y.**, **Zhang, Y.**, **Suhir, E. and Wang, X.** (2006). Thermal properties of carbon nanotube array used for integrated circuit cooling, *Journal of Applied Physics*, *100*(7), 074302.

[22] **Qin, Y.**, **Li, B. and Wang, S.** (2012). Experimental investigation of a novel polymeric heat exchanger using modified polypropylene hollow fibers, *Industrial & engineering chemistry research*, *51*(2), 882–890.

[23] **T'Joen, C.**, **Park, Y.**, **Wang, Q.**, **Sommers, A.**, **Han, X. and Jacobi, A.** (2009). A review on polymer heat exchangers for HVAC&R applications, *International journal of refrigeration*, *32*(5), 763–779.

[24] **Jia, L.**, **Peng, X.**, **Sun, J. and Chen, T.** (2001). An experimental study on vapor condensation of wet flue gas in a plastic heat exchanger, *Heat Transfer—Asian Research: Co-sponsored by the Society of Chemical Engineers of Japan and the Heat Transfer Division of ASME*, *30*(7), 571–580.

[25] **Sain, P.**, **Goyal, R.**, **Bhargava, A. and Prasad, Y.** (2013). Thermal and electronic behaviour of polycarbonate–copper nanocomposite system, *Journal of Physics D: Applied Physics*, *46*(45), 455501.

[26] **Kumlutaş, D.**, **Tavman, I.H. and Çoban, M.T.** (2003). Thermal conductivity of particle filled polyethylene composite materials, *Composites science and technology*, *63*(1), 113–117.

[27] **Boudenne, A.**, **Ibos, L.**, **Fois, M.**, **Majesté, J. and Géhin, E.** (2005). Electrical and thermal behavior of polypropylene filled with copper particles, *Composites Part A: Applied Science and Manufacturing*, *36*(11), 1545–1554.

[28] **Mamunya, Y.P.**, **Davydenko, V.**, **Pissis, P. and Lebedev, E.** (2002). Electrical and thermal conductivity of polymers filled with metal powders, *European polymer journal*, *38*(9), 1887–1897.

[29] **Chung, D.** (2001). Materials for thermal conduction, *Applied thermal engineering*, *21*(16), 1593–1605.

[30] **Zhao, Y.H.**, **Zhang, Y.F.**, **Bai, S.L. and Yuan, X.W.** (2016). Carbon fibre/graphene foam/polymer composites with enhanced mechanical and thermal properties, *Composites Part B: Engineering*, *94*, 102–108.

[31] **Stankovich, S.**, **Dikin, D.A.**, **Dommett, G.H.**, **Kohlhaas, K.M.**, **Zimney, E.J.**, **Stach, E.A.**, **Piner, R.D.**, **Nguyen, S.T. and Ruoff, R.S.** (2006). Graphene-based composite materials, *nature*, *442*(7100), 282–286.

[32] **Veca, L.M.**, **Meziani, M.J.**, **Wang, W.**, **Wang, X.**, **Lu, F.**, **Zhang, P.**, **Lin, Y.**, **Fee, R.**, **Connell, J.W. and Sun, Y.P.** (2009). Carbon nanosheets for polymeric nanocomposites with high thermal conductivity, *Advanced Materials*, *21*(20), 2088–2092.

[33] **Kim, P.**, **Shi, L.**, **Majumdar, A. and McEuen, P.L.** (2001). Thermal transport measurements of individual multiwalled nanotubes, *Physical review letters*, *87*(21), 215502.

[34] **Pizza, A.**, **Metz, R.**, **Hassanzadeh, M. and Bantignies, J.L.** (2014). Life cycle assessment of nanocomposites made of thermally conductive graphite nanoplatelets, *The International Journal of Life Cycle Assessment*, *19*(6), 1226–1237.

[35] **Singh, V.**, **Joung, D.**, **Zhai, L.**, **Das, S.**, **Khondaker, S.I. and Seal, S.** (2011). Graphene based materials: past, present and future, *Progress in materials science*, *56*(8), 1178–1271.

[36] **Zheng, Q.**, **Li, Z.**, **Yang, J. and Kim, J.K.** (2014). Graphene oxide-based transparent conductive films, *Progress in Materials Science*, *64*, 200–247.

[37] **Raman, C. and Meneghetti, P.** (2008). Boron nitride finds new applications in thermoplastic compounds, *Plastics, Additives and Compounding*, *10*(3), 26–31.

[38] **Leung, S.N.**, **Khan, M.O.**, **Chan, E.**, **Naguib, H.**, **Dawson, F.**, **Adinkrah, V. and Lakatos-Hayward, L.** (2013). Analytical modeling and characterization of heat transfer in thermally conductive polymer composites filled with spherical particulates, *Composites Part B: Engineering*, *45*(1), 43–49.

[39] **Wu, S.Y.**, **Huang, Y.L.**, **Ma, C.C.M.**, **Yuen, S.M.**, **Teng, C.C. and Yang, S.Y.** (2011). Mechanical, thermal and electrical properties of aluminum nitride/polyetherimide composites, *Composites Part A: Applied Science and Manufacturing*, *42*(11), 1573–1583.

[40] **Che, J.**, **Jing, M.**, **Liu, D.**, **Wang, K. and Fu, Q.** (2018). Largely enhanced thermal conductivity of HDPE/boron nitride/carbon nanotubes ternary composites via filler network-network synergy and orientation, *Composites Part A: Applied Science and Manufacturing*, *112*, 32–39.

[41] **Cheewawuttipong, W.**, **Fuoka, D.**, **Tanoue, S.**, **Uematsu, H. and Iemoto, Y.** (2013). Thermal and mechanical properties of polypropylene/boron nitride composites, *Energy Procedia*, *34*, 808–817.

[42] **Pak, S.Y.**, **Kim, H.M.**, **Kim, S.Y. and Youn, J.R.** (2012). Synergistic improvement of thermal conductivity of thermoplastic composites with mixed boron nitride and multi-walled carbon nanotube fillers, *Carbon*, *50*(13), 4830–4838.

[43] **Hwang, Y.**, **Kim, M. and Kim, J.** (2013). Improvement of the mechanical properties and thermal conductivity of poly (ether-ether-ketone) with the addition of graphene oxide-carbon nanotube hybrid fillers, *Composites Part A: Applied Science and Manufacturing*, *55*, 195–202.

[44] **Shin, Y.K.**, **Lee, W.S.**, **Yoo, M.J. and Kim, E.S.** (2013). Effect of BN filler on thermal properties of HDPE matrix composites, *Ceramics International*, *39*, S569–S573.

[45] **Li, T.L. and Hsu, S.L.C.** (2010). Enhanced thermal conductivity of polyimide films via a hybrid of micro-and nano-sized boron nitride, *The Journal of Physical Chemistry B*, *114*(20), 6825–6829.

[46] **Kim, H.S.**, **Jang, J.u.**, **Yu, J. and Kim, S.Y.** (2015). Thermal conductivity of polymer composites based on the length of multi-walled carbon nanotubes, *Composites Part B: Engineering*, *79*, 505–512.

[47] **Zhou, W.**, **Yu, D.**, **Wang, C.**, **An, Q. and Qi, S.** (2008). Effect of filler size distribution on the mechanical and physical properties of alumina-filled silicone rubber, *Polymer Engineering & Science*, *48*(7), 1381–1388.

[48] **Burger, N.**, **Laachachi, A.**, **Ferriol, M.**, **Lutz, M.**, **Toniazzo, V. and Ruch, D.** (2016). Review of thermal conductivity in composites: mechanisms, parameters and theory, *Progress in Polymer Science*, *61*, 1–28.

[49] **Karippal, J.J.**, **Murthy, H.N.**, **Rai, K.**, **Krishna, M. and Sreejith, M.** (2010). Electrical and thermal properties of twin-screw extruded multiwalled carbon nanotube/epoxy composites, *Journal of materials engineering and performance*, *19*(8), 1143–1149.

[50] **Song, Y.S. and Youn, J.R.** (2005). Influence of dispersion states of carbon nanotubes on physical properties of epoxy nanocomposites, *Carbon*, *43*(7), 1378–1385.

[51] **Patti, A.**, **Acierno, D. and Russo, P.** (2017). Influence of filler dispersion and interfacial resistance on thermal conductivity of polypropylene/carbon nanotubes systems, *AIP Conference Proceedings*, volume1914, AIP Publishing LLC, p.030014.

[52] **Zhou, W.**, **Qi, S.**, **Li, H. and Shao, S.** (2007). Study on insulating thermal conductive BN/HDPE composites, *Thermochimica Acta*, *452*(1), 36–42.

[53] **Wu, H. and Drzal, L.T.** (2013). High thermally conductive graphite nanoplatelet/polyetherimide composite by precoating: Effect of percolation and particle size, *Polymer composites*, *34*(12), 2148–2153.

[54] **Lee, H.L.**, **Kwon, O.H.**, **Ha, S.M.**, **Kim, B.G.**, **Kim, Y.S.**, **Won, J.C.**, **Kim, J.**, **Choi, J.H. and Yoo, Y.** (2014). Thermal conductivity improvement of surface-enhanced polyetherimide (PEI) composites using polyimide-coated h-BN particles, *Physical Chemistry Chemical Physics*, *16*(37), 20041–20046.

[55] **Jung, J.**, **Kim, J.**, **Uhm, Y.R.**, **Jeon, J.K.**, **Lee, S.**, **Lee, H.M. and Rhee, C.K.** (2010). Preparations and thermal properties of micro-and nano-BN dispersed HDPE composites, *Thermochimica acta*, *499*(1-2), 8–14.

[56] **Fisa, B.** (1985). Mechanical degradation of glass fibers during compounding with polypropylene, *Polymer composites*, *6*(4), 232–241.

[57] **Leung, S.N.** (2018). Thermally conductive polymer composites and nanocomposites: Processing-structure-property relationships, *Composites Part B: Engineering*, *150*, 78–92.

[58] **Kumar, S.**, **Sun, L.**, **Caceres, S.**, **Li, B.**, **Wood, W.**, **Perugini, A.**, **Maguire, R. and Zhong, W.** (2010). Dynamic synergy of graphitic nanoplatelets and multi-walled carbon nanotubes in polyetherimide nanocomposites, *Nanotechnology*, *21*(10), 105702.

[59] **Hwang, Y.**, **Heo, Y.**, **Yoo, Y. and Kim, J.** (2014). The addition of functionalized graphene oxide to polyetherimide to improve its thermal conductivity and mechanical properties, *Polymers for Advanced Technologies*, *25*(10), 1155–1162.

[60] **Ling, J.**, **Zhai, W.**, **Feng, W.**, **Shen, B.**, **Zhang, J. and Zheng, W.g.** (2013). Facile preparation of lightweight microcellular polyetherimide/graphene composite foams for electromagnetic interference shielding, *ACS applied materials & interfaces*, *5*(7), 2677–2684.

[61] **Caneba, G.**, **Dutta, C.**, **Agrawal, V.**, **Rao, M.** *et al.* (2010). Novel ultrasonic dispersion of carbon nanotubes, *Journal of Minerals and Materials Characterization and Engineering*, *9*(03), 165.

[62] **Chen, H.**, **Ginzburg, V.V.**, **Yang, J.**, **Yang, Y.**, **Liu, W.**, **Huang, Y.**, **Du, L. and Chen, B.** (2016). Thermal conductivity of polymer-based composites: Fundamentals and applications, *Progress in Polymer Science*, *59*, 41–85.

[63] **Kasap, S.** (2006). *Springer handbook of electronic and photonic materials*, Springer Science & Business Media.

[64] **Choy, C.** (1977). Thermal conductivity of polymers, *Polymer*, *18*(10), 984–1004.

[65] **Shen, S.**, **Henry, A.**, **Tong, J.**, **Zheng, R. and Chen, G.** (2010). Polyethylene nanofibres with very high thermal conductivities, *Nature nanotechnology*, *5*(4), 251–255.

[66] **Ng, H.Y.**, **Lu, X. and Lau, S.K.** (2005). Thermal conductivity of boron nitride-filled thermoplastics: effect of filler characteristics and composite processing conditions, *Polymer Composites*, *26*(6), 778–790.

[67] **Rapoport, L.**, **Feldman, Y.**, **Homyonfer, M.**, **Cohen, H.**, **Sloan, J.**, **Hutchison, J. and Tenne, R.** (1999). Inorganic fullerene-like material as additives to lubricants: structure–function relationship, *Wear*, *225*, 975–982.

[68] **Kordkheili, H.Y.**, **Farsi, M. and Rezazadeh, Z.** (2013). Physical, mechanical and morphological properties of polymer composites manufactured from carbon nanotubes and wood flour, *Composites Part B: Engineering*, *44*(1), 750–755.

[69] **Moniruzzaman, M. and Winey, K.I.** (2006). Polymer nanocomposites containing carbon nanotubes, *Macromolecules*, *39*(16), 5194–5205.

[70] **Chartoff, R.P. and Sircar, A.K.** (2002). Thermal analysis of polymers, *Encyclopedia of polymer science and technology*.

[71] **Sepe, M.P.** (1997). *Thermal analysis of polymers*, volume 95, iSmithers Rapra Publishing.

[72] **de Assumpção Pereira-da Silva, M. and Ferri, F.A.**, (2017). Scanning Electron Microscopy, Nanocharacterization Techniques, Elsevier, pp.1–35.

[73] **Singh, A.K.** (2016). Experimental methodologies for the characterization of nanoparticles, *Engineered nanoparticles*, *2*, 125–170.

[74] **Shaw, M.T.** (2012). *Introduction to polymer rheology*, Wiley Online Library.

[75] **Bylund, G.**, Dairy Processing Handbook, 2001.

[76] **Rauwendaal, C.** (2018). *Understanding extrusion*, Carl Hanser Verlag GmbH Co KG.

[77] **Xu, D. and Wang, Z.** (2008). Role of multi-wall carbon nanotube network in composites to crystallization of isotactic polypropylene matrix, *Polymer*, *49*(1), 330–338.

[78] **Xiao, Y.j.**, **Wang, W.y.**, **Chen, X.j.**, **Lin, T.**, **Zhang, Y.t.**, **Yang, J.h.**, **Wang, Y. and Zhou, Z.w.** (2016). Hybrid network structure and thermal conductive properties in poly (vinylidene fluoride) composites based on carbon nanotubes and graphene nanoplatelets, *Composites Part A: Applied Science and Manufacturing*, *90*, 614–625.

[79] **Ahn, H.J.**, **Eoh, Y.J.**, **Park, S.D. and Kim, E.S.** (2014). Thermal conductivity of polymer composites with oriented boron nitride, *Thermochimica Acta*, *590*, 138–144.

[80] **Zhang, Q.**, **Wu, G.**, **Jiang, L. and Chen, G.** (2003). Thermal expansion and dimensional stability of Al–Si matrix composite reinforced with high content SiC, *Materials Chemistry and Physics*, *82*(3), 780–785.

[81] **Ghose, S.**, **Working, D.C.**, **Connell, J.W.**, **Smith Jr, J.**, **Watson, K.A.**, **Delozier, D.M.**, **Sun, Y. and Lin, Y.** (2006). Thermal conductivity of ultemTM/carbon nanofiller blends, *High Performance Polymers*, *18*(6), 961–977.

[82] **Ren, P.G.**, **Yan, D.X.**, **Chen, T.**, **Zeng, B.Q. and Li, Z.M.** (2011). Improved properties of highly oriented graphene/polymer nanocomposites, *Journal of Applied Polymer Science*, *121*(6), 3167–3174.

[83] **Liu, M.**, **Du, Y.**, **Miao, Y.E.**, **Ding, Q.**, **He, S.**, **Tjiu, W.W.**, **Pan, J. and Liu, T.** (2015). Anisotropic conductive films based on highly aligned polyimide fibers containing hybrid materials of graphene nanoribbons and carbon nanotubes, *Nanoscale*, *7*(3), 1037–1046.

CURRICULUM VITAE

Name Surname: Yunus Emre BOZKURT

Place and Date of Birth: Istanbul, 23/01/1994

E-Mail: bozkurt.yun@gmail.com

EDUCATION:

- **B.Sc.:** 2018, Istanbul Technical University, Chemical and Metallurgical Engineering Faculty, Metallurgical and Materials Engineering Department

PUBLICATIONS, PRESENTATIONS AND PATENTS ON THE THESIS:

- **Bozkurt Y.E**, Kaynan O., Yildiz A., Ozden Y. E., Cebeci F. C., Cebeci H., Akar E., Kaygınok F., Kızılcık G., Solak N., 2019. BN/HDPE and BN/PEI Composites for Thermal Management Applications. *International Conference of The Polymer Processing Society*, 26-30 May, 2019 İzmir, Turkey. (Oral Presentation)

OTHER PUBLICATIONS, PRESENTATIONS AND PATENTS:

- Kaynan, O., Yıldız, A., **Bozkurt, Y. E.**, Yenigun, E. O., & Cebeci, H., "Electrically conductive high-performance thermoplastic filaments for fused filament fabrication," *Composite Structures, 237, 111930.*, 2020

- Kaynan, O., Yildiz, A., **Bozkurt, Y. E.**, Ozden Yenigun, E., & Cebeci, H. (2019). "Development of Multifunctional CNTs Reinforced PEI Filaments for Fused Deposition Modeling," *In AIAA Scitech Forum* (p. 0406), 2019